

Renormalized linear kinetic theory as derived from quantum field theory: A novel diagrammatic method for computing transport coefficients

Yoshimasa Hidaka and Teiji Kunihiro

Department of Physics, Kyoto University, Sakyo-ku, Kyoto 606-8502, Japan

(Received 7 October 2010; revised manuscript received 24 February 2011; published 6 April 2011)

We propose a novel diagrammatic method for computing transport coefficients in relativistic quantum field theory. The self-consistent equation for summing the diagrams with pinch singularities has the form of a linearized kinetic equation as usual, but our formalism enables us to incorporate higher-order corrections of the coupling systematically for the first time. Furthermore, it is clarified that the higher-order corrections are nicely summarized into that of the vertex function, spectral function, and collision term. We identify the diagrams up to the next-to-next-leading-order corrections in the weak coupling expansion of ϕ^4 theory, which is a difficult task in kinetic approaches and other diagrammatic methods.

DOI: [10.1103/PhysRevD.83.076004](https://doi.org/10.1103/PhysRevD.83.076004)

PACS numbers: 11.10.Wx, 12.38.Mh, 25.75.-q

I. INTRODUCTION

The experimental results of heavy ion collisions at the Relativistic Heavy Ion Collider (RHIC) brought remarkable results [1–4]. Among others, the elliptic flow in peripheral collisions suggests that the ratio of the shear viscosity to the entropy, η/s , is smaller than those ever observed in other systems [4,5]. Transport coefficients such as the shear η and the bulk ζ viscosities reflect dynamical properties slightly away from the thermal equilibrium, while pressure, entropy, susceptibility, etc., reflect static properties. In the kinetic theory, the shear viscosity is proportional to the mean free path of quasiparticles of a long life; a short mean free path corresponds to strongly interacting matter [6], which is the reason why the quark-gluon plasma at the RHIC is called a strongly coupled quark-gluon plasma [2]. In any event, the RHIC experiments and the subsequent analyses prompted a great interest in the relativistic quantum field theory for the transport coefficients or nonequilibrium dynamics, in general.

Formally, the transport coefficients are expressed by the so-called Kubo formula [7] in the framework of linear response theory even for the relativistic system; e.g., the shear and the bulk viscosities are given by

$$\eta = \frac{1}{10} \lim_{\omega \rightarrow 0} \frac{1}{\omega} \text{Im} \int d^4x e^{i\omega t} i\theta(t) \langle [\pi_{ij}(x), \pi^{ij}(0)] \rangle, \quad (1)$$

$$\zeta = \lim_{\omega \rightarrow 0} \frac{1}{\omega} \text{Im} \int d^4x e^{i\omega t} i\theta(t) \langle [\mathcal{P}(x), \mathcal{P}(0)] \rangle, \quad (2)$$

respectively, where $\mathcal{P}(x) = -T^i_i(x)/3$ and $\pi_{ij}(x) = T_{ij}(x) + g_{ij}\mathcal{P}(x)$. $T_{\mu\nu}(x)$ is the energy-momentum tensor. We work in Minkowski space with a metric, $g_{\mu\nu} = \text{diag}(1, -1, -1, -1)$. Although concisely expressed by the Kubo formula, the computation of the transport coefficients is not a simple task in practice.

Lattice QCD simulation, in principle, provides us with a powerful nonperturbative method, and it is natural that there are attempts to apply it to calculate transport

coefficients at a vanishing chemical potential [8–10]. However, one must notice that the calculation of the energy-momentum tensor on the lattice is not, by far, straightforward, because a more careful analysis would be necessary of the low-frequency structure of the spectral function and the relevant relaxation time scales which are to be extracted from the imaginary-time correlation function, as warned in [9].

Recently, calculations relying on gauge/gravity correspondence have become popular, in which the retarded correlation function can be calculated as the absorbed cross section of the black hole [11,12]. One of the most important results from such an approach is that the ratio of the shear viscosity to the entropy density in $\mathcal{N} = 4$ supersymmetric gauge theories is as small as $1/4\pi$ with an infinite number of colors and strong coupling, and this value is conjectured to be a universal lower bound [11,12].

Even with the recent development of the fancy methods for calculating the transport coefficients, the most reliable method with the sound basis in the relativistic quantum field theory would be a diagrammatic one based on the loop expansion. One of the most important and difficult parts of such a method is, however, how to implement a systematic way to deal with the so-called “pinch singularity,” which would make naive perturbation theory based on the loop expansion break down. In fact, this difficulty could be overcome by a resummation of specific ladder diagrams. Although restricted to the leading order of a coupling constant or large N expansion, several methods for such a resummation have been proposed [13–17], and their outcome has been shown to be equivalent to the results obtained using the relativistic kinetic or Boltzmann equation within the leading order of a coupling constant [13,17]. We here remark that direct applications of relativistic kinetic theories are also done to compute the transport coefficients in the hadronic [18], quark-gluon plasma [19,20], and the “semiquark-gluon plasma” phases [21].

The merit of the diagrammatic methods based on the loop expansion over the direct use of the Boltzmann

equation is the potential ability to take into account the higher-order effects of the coupling constant systematically, in principle. As far as we know, there were, however, only a few works which were able to examine the next leading order for a relativistic system, still being confined to a scalar theory [22,23]. The major technical difficulty for going beyond the leading order of the coupling constant is to classify diagrams order-by-order in the coupling constant, because the loop expansion no longer corresponds to the coupling expansion at finite temperature and/or density.

The purpose of this paper is to give a formulation for a novel resummation method in which transport coefficients can be calculated systematically for any order of the coupling constant beyond the leading order for a relativistic system. Our method is motivated by the Eliashberg theory for a nonrelativistic system [24] like a Fermi liquid, although it relies on a cumbersome analytic continuation inherent in the imaginary-time formalism adopted by Eliashberg. We extend and reformulate the resummation method developed by Eliashberg to relativistic quantum field theory at high temperature. One of our ideas is to employ the real-time formalism to avoid the complicated analytical continuation and thus make the calculational procedure transparent. The real-time formalism is also found convenient for identifying diagrams corresponding to the pinch singularity, as will be discussed in Sec. IV.

The paper is organized as follows: In Sec. II, we briefly review why the difficulty arises when computing the transport coefficients. In Sec. III, we review the real-time formalism in the R/A basis that is useful for identifying the dominant diagrams in the Green function corresponding to the transport coefficient. In Sec. IV, the computation method for transport coefficients is discussed, and we show that the resummation equation has a form similar to a linearized Boltzmann equation. In Sec. V, we will conclude the paper with some outlook.

II. PINCH SINGULARITY AND QUASIPARTICLES

The difficulty in computing transport coefficients in Eqs. (1) and (2) arises from the infrared limit, $\omega \rightarrow 0$, of the Green function corresponding to a long time scale. In such long time scales, a lot of microscopic scatterings occur. In a diagrammatic method, such scatterings are expressed by multiple loop diagrams. The question is, what kind of diagrams are dominating and should be resummed? A particle excitation of a long life is called a quasiparticle, and, as long as the quasiparticle description is valid for the system under consideration, thermal excitations of the system will be well-described solely by the quasiparticle excitations. Such an excitation is expressed by a product of the retarded and advanced Green functions of the quasiparticles, which product is found to become divergent in the infinite lifetime limit. This divergence or singularity is nothing but the pinch singularity that we mentioned in the Introduction.

To see this more concretely, let us take the ϕ^4 theory, in which the one-particle retarded and advanced propagator reads

$$D^R(k) = \frac{-1}{k^2 - m^2 - \text{Re}\Pi_R(k) - i\text{Im}\Pi_R(k)} = D^{A^*}(k), \quad (3)$$

where m is the mass of the scalar particle, and $\Pi_R(k)$ is the retarded self-energy. These propagators can be approximated by a sum of poles corresponding to quasiparticle excitations, and thus we have

$$D^R(k) \simeq \sum_n \frac{-z_n(\mathbf{k})}{k^0 - \epsilon_n(\mathbf{k}) + i\gamma_n(\mathbf{k})}, \quad (4)$$

$$D^A(k) \simeq \sum_n \frac{-z_n^*(\mathbf{k})}{k^0 - \epsilon_n(\mathbf{k}) - i\gamma_n(\mathbf{k})}, \quad (5)$$

where $\epsilon_n(\mathbf{k})$ is the energy of the quasiparticle, $z_n(\mathbf{k})$ the renormalization function, and $\gamma_n(\mathbf{k}) > 0$ the damping rate. At weak coupling and high temperature ($m \ll \lambda T$), $\epsilon_n(\mathbf{k}) \simeq \pm\sqrt{k^2 + m_T^2}$, with the thermal mass defined in Eq. (89) below, and $z_n(\mathbf{k}) \simeq 1/(2|\epsilon_n(\mathbf{k})|)$. The damping rate owing to $2 \rightarrow 2$ scattering is of order $\lambda^2 T$. In the naive perturbation theory, one would encounter a product of the retarded and the advanced propagators, $D^R(p+k)D^A(k)$, which has the following anomalous behavior at small p under the quasiparticle approximation

$$D^R(p+k)D^A(k) \simeq 2\pi i \sum_n \frac{|z_n(\mathbf{k})|^2}{p^0 - \mathbf{v}_n \cdot \mathbf{p} + 2i\gamma_n(\mathbf{k})} \times \delta(k^0 - \epsilon_n(\mathbf{k})), \quad (6)$$

where $\mathbf{v}_n = d\epsilon_n(\mathbf{k})/d\mathbf{k}$ is the velocity of the quasiparticle. Equation (6) shows that, when the damping rate vanishes, i.e., $\gamma_n(\mathbf{k}) = 0$, the product diverges at $p = 0$; this is the pinch singularity as mentioned above. And one sees that the product of the retarded and the advanced propagators with the common momentum must be summed over to have a sensible result.

The need for resummation can be seen even apart from the quasiparticle approximation. The product of the propagators at $p = 0$ exactly becomes

$$\lim_{p \rightarrow 0} D^R(p+k)D^A(k) = \frac{\rho(k)}{-2\text{Im}\Pi_R(k)}, \quad (7)$$

where $\rho(k)$ is the spectral function defined by

$$\begin{aligned} \rho(k) &\equiv 2\text{Im}D^R(k) \\ &= \frac{-2\text{Im}\Pi_R(k)}{(k^2 - m^2 - \text{Re}\Pi_R(k))^2 + (\text{Im}\Pi_R(k))^2}. \end{aligned} \quad (8)$$

One sees that Eq. (7) diverges when the imaginary part of the self-energy vanishes. Therefore, we have to employ the dressed propagator, Eq. (3), to avoid the singularity.

III. REAL-TIME FORMALISM

In this section, we briefly review the real-time formalism [25]. For simplicity, we consider the ϕ^4 theory. The Lagrangian has the form

$$\mathcal{L} = \frac{1}{2}(\partial_\mu \phi)^2 - \frac{m^2}{2}\phi^2 - \frac{\lambda}{4!}\phi^4. \quad (9)$$

The real-time formalism is formulated on a complex-time path, shown in Fig. 1. The fields on C_1 and C_2 are called the type-1 field, ϕ^1 , and the type-2 field, ϕ^2 , respectively. The partition function is

$$\begin{aligned} Z_{12} = & \int \mathcal{D}\phi^1 \mathcal{D}\phi^2 \exp\left[-\frac{1}{2} \int d^4x d^4x' \phi^a(x) \right. \\ & \times D_{F,ab}^{-1}(x, x') \phi^b(x') - i \int d^4x (\mathcal{V}(\phi^1) - \mathcal{V}(\phi^2)) \left. \right]. \end{aligned} \quad (10)$$

Although there are contributions from the paths C_3 and C_4 , in general, they are factorized in the limit of $t_i, t_f \rightarrow \infty$, and are irrelevant as long as correlation functions are concerned [25]. The free propagators in momentum space read

$$\begin{aligned} D_F^{11} &= (1 + n(k^0))D_F(k) + n(k^0)D_F^*(k), \\ D_F^{12} &= e^{\sigma k^0}(n(k^0) + \theta(-k^0))(D_F(k) + D_F^*(k)), \\ D_F^{21} &= e^{-\sigma k^0}(n(k^0) + \theta(k^0))(D_F(k) + D_F^*(k)), \\ D_F^{22} &= (1 + n(k^0))D_F^*(k) + n(k^0)D_F(k), \end{aligned} \quad (11)$$

where the σ is the parameter characterizing the time path in Fig. 1, $D_F(k)$ is the free Feynman propagator defined by

$$D_F(k) = \frac{i}{k^2 - m^2 + i\epsilon}, \quad (12)$$

and $n(k^0)$ is the Bose-Einstein distribution function,

$$n(k^0) = \frac{1}{e^{\beta|k^0|} - 1}, \quad (13)$$

with inverse temperature $\beta = 1/T$. We note that any physical observable is independent of the choice of the path, i.e., σ .

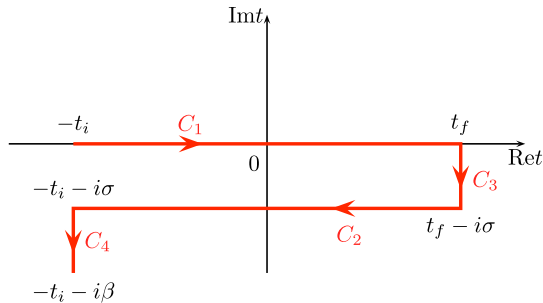


FIG. 1 (color online). A complex-time path in the real-time formalism.

For later convenience, let us rewrite Eq. (11) in terms of the retarded and advanced propagators,

$$\begin{aligned} D_F^{11}(k) &= (1 + f(k^0))(-iD_F^R(k) + f(k^0)(iD_F^A(k)), \\ D_F^{12}(k) &= e^{\sigma k^0} f(k^0)(-iD_F^R(k) + iD_F^A(k)), \\ D_F^{21}(k) &= e^{-\sigma k^0} (1 + f(k^0))(-iD_F^R(k) + iD_F^A(k)), \\ D_F^{22}(k) &= f(k^0)(-iD_F^R(k) + (1 + f(k^0))(iD_F^A(k)), \end{aligned} \quad (14)$$

where the free retarded and advanced propagators are defined by

$$D_F^R(k) \equiv \frac{-1}{k^2 - m^2 + i\epsilon k^0}, \quad (15)$$

$$D_F^A(k) \equiv \frac{-1}{k^2 - m^2 - i\epsilon k^0}, \quad (16)$$

and $f(k^0)$ is defined as

$$f(k^0) \equiv \frac{1}{e^{\beta k^0} - 1}. \quad (17)$$

These propagators satisfy $D_F^R(-k) = D_F^R(k) = D_F^A(k)$, which relation also holds for the full propagators (see Appendix A). The relation between the Bose-Einstein distribution function and $f(k^0)$ is $n(k^0) = f(|k^0|)$.

R/A basis

In this subsection, we introduce a useful basis called the “R/A basis” for computing transport coefficients [26,27]. In the original representation introduced by Aurenche and Becherrawy [26], the propagators are diagonal, and the diagonal components are the retarded and advanced propagators. In the present work, rather, we employ the representation in which the diagonal components are zero while the off-diagonal components are not [27], instead of the original R/A basis (we also refer this as the R/A basis in this paper). We find that this basis is useful not only for a comparison of the real-time correlation function obtained in the real-time formalism with that in the imaginary time but also for the identification of pinch singularities.

Let us define a rotation matrix for converting the basis Eq. (11) (we refer to this basis as the “standard basis”) to the R/A basis in momentum space as

$$\phi^\alpha(k) = U^\alpha_a(k)\phi^a(k), \quad (18)$$

where the Greek index denotes R or A, and the Latin index denotes 1 or 2. We use Einstein notation, i.e., if an index appears twice in a single term, once as a superscript and once as subscript, a summation is assumed over all of its possible values. We also define the metric for the standard basis as $g_{ab} = g^{ab} \equiv \text{diag}(1, -1)$; then, the metric in the R/A basis is given by $g_{\alpha\beta} = g_{ab}U^\alpha_a(k)U^\beta_b(-k)$, of which the explicit form is given below. The inverse matrix $U^\beta_\alpha(k)$ is defined by $\delta^b_a = U^\beta_\alpha(k)U^\alpha_b(k)$. An n -point function transforms as a tensor:

$$\Gamma_{\alpha\beta\dots}(k_1, k_2, \dots) = \Gamma_{ab\dots}(k_1, k_2, \dots) U^a_{\alpha}(k_1) U^b_{\beta}(k_2) \dots, \quad (19)$$

$$D^{\alpha\beta\dots}(k_1, k_2, \dots) = D^{ab\dots}(k_1, k_2, \dots) U^a_{\alpha}(k_1) U^b_{\beta}(k_2) \dots. \quad (20)$$

In particular, the propagator or two-point function transforms as

$$D^{ab}(k) = U^a_{\alpha}(k) U^b_{\beta}(-k) D^{\alpha\beta}(k). \quad (21)$$

In the R/A basis, $D^{\alpha\beta}(k)$ is chosen so that the diagonal part vanishes:

$$\begin{aligned} D^{\alpha\beta}(k) &= \begin{pmatrix} D^{RR}(k) & D^{RA}(k) \\ D^{AR}(k) & D^{AA}(k) \end{pmatrix} \\ &= \begin{pmatrix} 0 & -iD^R(k) \\ -iD^A(k) & 0 \end{pmatrix}. \end{aligned} \quad (22)$$

The most general form of $U^a_{\alpha}(k)$ satisfying Eq. (22) is obtained through comparison with Eq. (14):

$$\begin{aligned} U^a_{\alpha}(k) &= \begin{pmatrix} U^1_R(k) & U^1_A(k) \\ U^2_R(k) & U^2_A(k) \end{pmatrix} \\ &= \begin{pmatrix} f(k^0) e^{\sigma k^0} c(k) & e^{(\sigma-\beta)k^0} / c(-k) \\ f(k^0) c(k) & 1/c(-k) \end{pmatrix}, \end{aligned} \quad (23)$$

where $c(k)$ is an arbitrary function. Here, we simply fix $c(k)$ to be constant, $c(k) = 1$, while the σ is kept to be a free parameter. Then,

$$U^a_{\alpha}(k) = \begin{pmatrix} f(k^0) e^{\sigma k^0} & e^{(\sigma-\beta)k^0} \\ f(k^0) & 1 \end{pmatrix}, \quad (24)$$

and the inverse is

$$\begin{aligned} U^{\alpha}_a(k) &= \begin{pmatrix} U^R_1(k) & U^R_2(k) \\ U^A_1(k) & U^A_2(k) \end{pmatrix} \\ &= \begin{pmatrix} e^{(\beta-\sigma)k^0} & -1 \\ -(1+f(k^0))e^{-\sigma k^0} & (1+f(k^0)) \end{pmatrix}. \end{aligned} \quad (25)$$

The metric in the R/A basis is

$$g_{\alpha\beta} = g_{ab} U^a_{\alpha}(k) U^b_{\beta}(-k) = \begin{pmatrix} 0 & 1 \\ 1 & 0 \end{pmatrix} = g^{\alpha\beta}, \quad (26)$$

which is independent of σ . The propagator can be rewritten by using the metric $g^{\alpha\beta}$:

$$D^{\alpha\beta}(k) = -i g^{\alpha\beta} D^{\alpha}(k), \quad (27)$$

with no sum over α . Here, we define the Feynman rule for the propagators with arrows:

$$\begin{array}{c} \text{---} \longleftarrow \text{---} \\ \longleftarrow k \end{array} = -i D^R(k), \quad (28)$$

$$\begin{array}{c} \text{---} \longrightarrow \text{---} \\ \longleftarrow k \end{array} = -i D^A(k) = -i D^R(-k). \quad (29)$$

The propagator is identified with $D^R(k)$ or $D^A(k)$, if the arrow is parallel or antiparallel to the momentum k , respectively. The four-point vertex transforms as

$$\begin{aligned} \lambda_{\alpha\beta\gamma\delta}(k_1, k_2, k_3, k_4) &= \lambda_{abcd} U^a_{\alpha}(k_1) U^b_{\beta}(k_2) \\ &\quad \times U^c_{\gamma}(k_3) U^d_{\delta}(k_4), \end{aligned} \quad (30)$$

where $\lambda_{abcd} = +\lambda$ if $a = b = c = d = 1$, and $\lambda_{abcd} = -\lambda$ if $a = b = c = d = 2$; otherwise, $\lambda_{abcd} = 0$. The vertex satisfies the energy-momentum conservation, $k_1 + k_2 + k_3 + k_4 = 0$. After simple calculations, one finds

$$\begin{aligned} \lambda_{\alpha\beta\gamma\delta}(k_1, k_2, k_3, k_4) &= \lambda [(1 + f(k_1^0))^{\delta_{\alpha R}} (1 + f(k_2^0))^{\delta_{\beta R}} \\ &\quad \times (1 + f(k_3^0))^{\delta_{\gamma R}} (1 + f(k_4^0))^{\delta_{\delta R}} \\ &\quad - (f(k_1^0))^{\delta_{\alpha R}} (f(k_2^0))^{\delta_{\beta R}} (f(k_3^0))^{\delta_{\gamma R}} (f(k_4^0))^{\delta_{\delta R}}]. \end{aligned} \quad (31)$$

The first and second terms in the right-hand side (rhs) correspond to the loss and the gain terms, respectively. The four-point vertex generally contains 16 combinations; however, thanks to the symmetry of the ϕ^4 theory, they reduce to the following five vertices:

$$\begin{array}{c} \begin{array}{c} \nearrow k_3 \\ \nwarrow k_2 \\ \swarrow k_4 \\ \searrow k_1 \end{array} \end{array} = -i \lambda_{RRRR}(k_1, k_2, k_3, k_4) = 0, \quad (32)$$

$$\begin{array}{c} \begin{array}{c} \nearrow \quad \quad \quad \nearrow \\ \nwarrow \quad \quad \quad \nwarrow \\ \swarrow \quad \quad \quad \swarrow \\ \searrow \quad \quad \quad \searrow \end{array} \end{array} = -i \lambda_{RRRA}(k_1, k_2, k_3, k_4) \\ = -i \lambda \left[(1 + f(k_1^0)) (1 + f(k_2^0)) (1 + f(k_3^0)) \right. \\ \left. - f(k_1^0) f(k_2^0) f(k_3^0) \right], \quad (33)$$

$$\begin{array}{c} \begin{array}{c} \nwarrow \quad \quad \quad \nwarrow \\ \nearrow \quad \quad \quad \nearrow \\ \swarrow \quad \quad \quad \swarrow \\ \searrow \quad \quad \quad \searrow \end{array} \end{array} = -i \lambda_{RRAA}(k_1, k_2, k_3, k_4) \\ = -i \lambda \left[(1 + f(k_1^0)) (1 + f(k_2^0)) \right. \\ \left. - f(k_1^0) f(k_2^0) \right], \quad (34)$$

$$\begin{array}{c} \begin{array}{c} \nwarrow \quad \quad \quad \nearrow \\ \nearrow \quad \quad \quad \nwarrow \\ \swarrow \quad \quad \quad \swarrow \\ \searrow \quad \quad \quad \searrow \end{array} \end{array} = -i \lambda_{RAAA}(k_1, k_2, k_3, k_4) = -i \lambda, \quad (35)$$

$$\begin{array}{c} \begin{array}{c} \nwarrow \quad \quad \quad \nearrow \\ \nearrow \quad \quad \quad \nwarrow \\ \swarrow \quad \quad \quad \swarrow \\ \searrow \quad \quad \quad \searrow \end{array} \end{array} = -i \lambda_{AAAA}(k_1, k_2, k_3, k_4) = 0. \quad (36)$$

At the tree level, vertices with all the same indices vanish, i.e., $\lambda_{RRRR} = \lambda_{AAAA} = 0$. This relation is satisfied in full n -point vertex functions; see Appendix A for the derivation. We should note, however, that this vanishment will no longer be maintained for the system out of equilibrium, where the Kubo-Martin-Schwinger condition is not satisfied [28].

IV. COMPUTATION METHOD FOR TRANSPORT COEFFICIENTS

In this section, we discuss the computational procedure for transport coefficients in the R/A basis and derive a self-consistent equation, which turns out to be an extension of the linearized Boltzmann equation. We shall see that the R/A basis can naturally lead to a decomposition of diagrams into the dominant diagrams, including pinch poles and others.

A. One-loop analysis

We shall start with the one-loop diagram of a retarded function. Here, we employ the dressed propagators, $D^R(k)$ and $D^A(k)$, which do not have a pinch singularity. We assume that the relevant operator $\mathcal{O}(x)$ to the transport coefficient is a quadratic one. The retarded Green function of it reads

$$\mathcal{G}_R^{\mathcal{O}}(p) = \int d^4x e^{ip \cdot x} i\theta(t) \langle [\mathcal{O}(x), \mathcal{O}(0)] \rangle. \quad (37)$$

At one-loop level,

$$\begin{aligned} \mathcal{G}_R^{\mathcal{O}}(p) &= \frac{i}{2} \int \frac{d^4k}{(2\pi)^4} \Gamma_{A\beta_1\alpha_1}^{(0)}(-p, -k, p+k) \\ &\quad \times D^{\alpha_1\alpha_2}(p+k) D^{\beta_1\beta_2}(-k) \Gamma_{R\alpha_2\beta_2}^{(0)}(p, -p-k, k), \end{aligned} \quad (38)$$

where the overall of $1/2$ is a symmetric factor, and the Feynman diagram for the vertex function, $\Gamma_{\alpha\beta\gamma}^{(0)}(k_1, k_2, k_3)$, corresponding to $\mathcal{O}(x)$, is given by

$$\begin{aligned} \begin{array}{c} \text{Diagram 1: A vertex with three incoming lines labeled } k_1, k_2, k_3 \text{ and one outgoing line.} \\ \text{Diagram 2: A vertex with three incoming lines labeled } k_1, k_2, k_3 \text{ and one outgoing line.} \end{array} \\ = \Gamma_{ARR}^{(0)}(k_1, k_2, k_3) \\ = \Gamma^{(0)}(k_1, k_2, k_3) (1 + f(k_2^0) + f(k_3^0)), \end{aligned} \quad (39)$$

$$\begin{array}{c} \text{Diagram 3: A vertex with three incoming lines labeled } k_1, k_2, k_3 \text{ and one outgoing line.} \\ = \Gamma_{AAR}^{(0)}(k_1, k_2, k_3) = \Gamma^{(0)}(k_1, k_2, k_3), \end{array} \quad (40)$$

and $\Gamma_{RRR}^{(0)}(k_1, k_2, k_3) = \Gamma_{AAA}^{(0)}(k_1, k_2, k_3) = 0$. For example, $\Gamma^{(0)}(k_1, k_2, k_3) = k_2^i k_3^j + k_3^i k_2^j - 2\delta^{ij} \mathbf{k}_2 \cdot \mathbf{k}_3 / 3$, for the

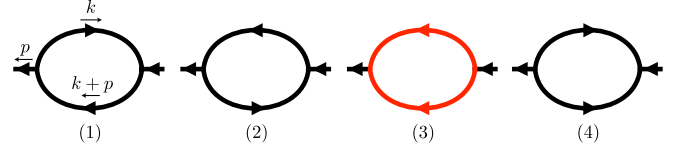


FIG. 2 (color online). One-loop diagram for a retarded Green function. The red (light gray) line corresponds to the product of the retarded and advanced propagators.

shear viscosity, where $\mathcal{O}(x) \propto \pi_{ij}(x)$. There are, in general, four diagrams shown in Fig. 2 contributing to the retarded Green function. Part (4) of the diagram vanishes because the vertex functions are $\Gamma_{RRR}^{(0)}(k_1, k_2, k_3) = \Gamma_{AAA}^{(0)}(k_1, k_2, k_3) = 0$. Part (1) of the diagram is expressed as

$$\begin{aligned} \mathcal{G}_R^{\mathcal{O}(1)}(p) &= \frac{i}{2} (-i)^2 \int \frac{d^4k}{(2\pi)^4} (1 + f(p^0) + f(k^0)) \\ &\quad \times \Gamma^{(0)}(-p, -k, p+k) D^R(k) D^R(p+k) \\ &\quad \times \Gamma^{(0)}(p, -p-k, k) \\ &= -\frac{i}{2} \int \frac{d^4k}{(2\pi)^4} f(k^0) \Gamma^{(0)}(-p, -k, p+k) \\ &\quad \times \Gamma^{(0)}(p, -p-k, k) D^R(k) D^R(p+k), \end{aligned} \quad (41)$$

where we have dropped the term proportional to $1 + f(p^0)$ that does not contain poles in the complex k^0 plane, since the vertex and the retarded propagator have no poles in the upper complex k^0 plane; the k^0 integral becomes zero. For a transport coefficient, we need the soft-momentum limit as

$$\begin{aligned} \sigma^{(1)} &\equiv \lim_{p^0 \rightarrow 0} \lim_{p \rightarrow 0} \frac{1}{p^0} \text{Im} \mathcal{G}_R^{\mathcal{O}(1)}(p) \\ &= \frac{1}{4} \int \frac{d^4k}{(2\pi)^4} \frac{\partial}{\partial k^0} f(k^0) \\ &\quad \times (\Gamma^{(0)}(0, k, -k))^2 \text{Re}(D^R(k))^2. \end{aligned} \quad (42)$$

For the contribution $\mathcal{G}_R^{\mathcal{O}(2)}(p)$ from part (2) of the diagram, one finds $\sigma^{(2)} = \sigma^{(1)}$. The contribution $\mathcal{G}_R^{\mathcal{O}(3)}(p)$ from part (3) of the diagram includes a product of the retarded and advanced propagators:

$$\begin{aligned} \mathcal{G}_R^{\mathcal{O}(3)}(p) &= \frac{i}{2} (-i)^2 \int \frac{d^4k}{(2\pi)^4} (1 + f(-k^0) + f(p^0 + k^0)) \\ &\quad \times D^A(k) D^R(p+k) \Gamma^{(0)}(-p, -k, p+k) \\ &\quad \times \Gamma^{(0)}(p, -p-k, k) \\ &= -\frac{i}{2} \int \frac{d^4k}{(2\pi)^4} (f(p^0 + k^0) - f(k^0)) \\ &\quad \times D^A(k) D^R(p+k) \Gamma^{(0)}(-p, -k, p+k) \\ &\quad \times \Gamma^{(0)}(p, -p-k, k). \end{aligned} \quad (43)$$

Then, the transport coefficient $\sigma^{(3)}$, due to $\mathcal{G}_R^{\mathcal{O}(3)}(p)$, becomes

$$\begin{aligned}\sigma^{(3)} &\equiv \lim_{p^0 \rightarrow 0} \lim_{p \rightarrow 0} \frac{1}{p^0} \text{Im} \mathcal{G}_R^{\mathcal{O}(3)}(p) \\ &= -\frac{1}{2} \int \frac{d^4 k}{(2\pi)^4} \frac{\partial}{\partial k^0} f(k^0) \frac{\rho(k)}{-2\text{Im}\Pi_R(k)} (\Gamma^{(0)}(0, k, -k))^2.\end{aligned}\quad (44)$$

If one uses the quasiparticle approximation, $\rho(k) = 2\pi\epsilon(k^0)\delta((k^0)^2 - E_k^2)$ and $\gamma_k = -\text{Im}\Pi_R(E_k, \mathbf{k})/(2E_k)$, $\sigma^{(3)}$ becomes

$$\sigma^{(3)} \simeq \frac{1}{T} \int \frac{d^3 k}{(2\pi)^3} f(E_k)(1 + f(E_k)) \frac{1}{2\gamma_k} \left(\frac{\Gamma^{(0)}(0, k, -k)}{2E_k} \right)^2, \quad (45)$$

while $\sigma^{(1)}$ and $\sigma^{(2)}$ vanish in this limit. At weak coupling, the decay width is proportional to λ^2 , so that $\sigma^{(3)} \sim 1/\lambda^2$. This gives the correct coupling dependence, but not the coefficient. The higher-order diagram contributes to the transport coefficient in the same order as the one-loop diagram.

Since the Bose-Einstein distribution function diverges at $k^0 = 0$, each $\mathcal{G}_R^{\mathcal{O}(i)}(p)$ includes divergence, although the sum of $\mathcal{G}_R^{\mathcal{O}(i)}(p)$'s is finite. In order to avoid such an artificial divergence, we introduce an infrared (IR) cutoff κ . Bosons with very soft momenta can no longer be regarded as particles, so we have to treat them, rather, as waves. This IR cutoff κ separates the scale between the particle and the wave. Thus, we take the IR scale to be $\kappa \ll m$. If one applies the quasiparticle approximation, the $\Pi_R(k)$ become independent of κ , because $k^0 \geq m \gg \kappa$ at the on shell of the quasiparticle. We note that a fermion

has no such a divergence because of the Fermi-Dirac distribution function.

The merit of the R/A basis is that it enables us to identify the diagrams with large contribution to $\mathcal{G}_R^{\mathcal{O}(3)}(p)$. Although such an identification and decomposition are not obvious in the imaginary-time formalism before the analytical continuation, the decomposition plays an important role for the full analysis of the retarded Green function, as is discussed in the next subsection.

B. Relativistic Eliashberg decomposition in real-time formalism

In the previous section, we showed within the one-loop level that the product of the retarded and advanced propagators with the common momentum gives a large contribution to transport coefficients. Such a product of the propagators also appears in higher-order diagrams, which must also be summed over. The Eliashberg method [24] is one such resummation method for nonrelativistic systems and has been applied to a Fermi liquid at low temperature in the imaginary-time formalism. In this method, the four-point function is first analytically continued to the real-time domain. Each external leg can be the retarded or advanced legs, so the four-point function has a matrix form. After the analytic continuation, the diagrams for the four-point function are decomposed into a set that connects with pinching diagrams and a set that does not connect with them. The pinching diagrams are summed over by a self-consistent equation, which is found to correspond to a kinetic equation. In this section, we extend the Eliashberg method to a relativistic case, using the real-time formalism in the R/A basis, and thus derive the corresponding relativistic kinetic equation.

The retarded Green function shown diagrammatically in Fig. 3 is expressed in the momentum space as

$$\begin{aligned}\mathcal{G}_R^{\mathcal{O}}(p) &= \int d^4 x e^{ip \cdot x} i\theta(t) \langle [\mathcal{O}(x), \mathcal{O}(0)] \rangle \\ &= \frac{i}{2} \int \frac{d^4 k}{(2\pi)^4} \int \frac{d^4 k'}{(2\pi)^4} \Gamma_{A\beta_1\alpha_1}^{(0)}(-p, -k, p+k) D^{\alpha_1\alpha_2}(p+k) D^{\beta_1\beta_2}(-k) [(2\pi)^4 \delta^{(4)}(k-k') \delta_{\alpha_2\alpha_4} \delta_{\beta_2\beta_4} \\ &\quad + (-i) \mathcal{T}_{\alpha_2\beta_2\beta_3\alpha_3}(-p-k, k, -k', p+k') D^{\alpha_3\alpha_4}(p+k') D^{\beta_3\beta_4}(-k')] \Gamma_{R\alpha_4\beta_4}^{(0)}(p, -p-k', k'),\end{aligned}\quad (46)$$

where $\mathcal{T}_{\alpha_2\beta_2\beta_3\alpha_3}(-p-k, k, -k', p+k')$ denotes the connected four-point function. The first diagram in the rhs of Fig. 3 is the one discussed in the previous subsection. Owing to Eq. (27), the product of two propagators appearing in Eq. (46) is written as

$$\begin{aligned}D^{\alpha_1\alpha_2}(p+k) D^{\beta_1\beta_2}(-k) \\ &= (-i)^2 g^{\alpha_1\alpha_2} g^{\beta_1\beta_2} D^{\alpha_1}(p+k) D^{\beta_1}(-k) \\ &\equiv -g^{\alpha_1\alpha_2} g^{\beta_1\beta_2} G^{\alpha_1\beta_1}(p, k).\end{aligned}\quad (47)$$

Thus, we have

$$\begin{aligned}\mathcal{G}_R^{\mathcal{O}}(p) &= -\frac{i}{2} \int \frac{d^4 k}{(2\pi)^4} \int \frac{d^4 k'}{(2\pi)^4} \Gamma_{A\beta_1\alpha_1}^{(0)}(-p, -k, p+k) \\ &\quad \times G^{\alpha_1\beta_1}(p, k) [(2\pi)^4 \delta^{(4)}(k-k') \delta_{\alpha_2\alpha_4} \delta_{\beta_2\beta_4} \\ &\quad + i \mathcal{T}_{\alpha_2\beta_2\beta_3\alpha_3}(-p-k, k, -k', p+k') \\ &\quad \times G^{\alpha_2\beta_2}(p, k')] \Gamma_{R\alpha_4\beta_4}^{(0)}(p, -p-k', k').\end{aligned}\quad (48)$$

$$\mathcal{G}_R^O(p) = \text{loop} + \text{loop with blue square}$$

FIG. 3 (color online). A retarded Green function corresponding to a transport coefficient. The dark (blue) square denotes the connected four-point function. The lines without arrows denote lines that can be the retarded or the advanced arrow lines.

The indices appear in pairs of α and β in Eq. (48), so it is useful to introduce an index l as the pairs of R and/or A , i.e., $l = (\alpha, \beta) = (RA), (AR), (RR),$ and (AA) ; then,

$$\begin{aligned} \mathcal{G}_R^O(p) = & -\frac{i}{2} \int \frac{d^4 k}{(2\pi)^4} \int \frac{d^4 k'}{(2\pi)^4} \Gamma_{Al}^{(0)}(p, k) G^l(p, k) \\ & \times [(2\pi)^4 \delta^{(4)}(k - k') \delta_m^l \\ & + i \mathcal{T}_m^l(p, k, k') G^m(p, k')] \Gamma_R^{(0)m}(p, k'), \quad (49) \end{aligned}$$

where the three-point functions are

$$\begin{aligned} \text{Diagram} & = \Gamma_R^{(0)1}(p, k) \\ & = \Gamma^{(0)}(p, -p - k, k) (1 + f(p^0) + f(k^0)), \quad (50) \end{aligned}$$

$$\begin{aligned} \text{Diagram} & = \Gamma_R^{(0)2}(p, k) \\ & = \Gamma^{(0)}(p, -p - k, k) \\ & \quad \times (f(p^0) - f(p^0 + k^0)), \quad (51) \end{aligned}$$

$$\begin{aligned} \text{Diagram} & = \Gamma_R^{(0)3}(p, k) = \Gamma^{(0)}(p, -p - k, k), \quad (52) \end{aligned}$$

$$\begin{aligned} \text{Diagram} & = \Gamma_{A1}^{(0)}(p, k) = \Gamma^{(0)}(-p, -k, p + k), \quad (53) \end{aligned}$$

$$\begin{aligned} \text{Diagram} & = \Gamma_{A2}^{(0)}(p, k) = \Gamma^{(0)}(-p, -k, p + k), \quad (54) \end{aligned}$$

$$\begin{aligned} \text{Diagram} & = \Gamma_{A3}^{(0)}(p, k) \\ & = \Gamma^{(0)}(-p, -k, p + k) (f(p^0 + k^0) - f(k^0)), \end{aligned}$$

and $\Gamma_{R4}^{(0)}(p, k) = \Gamma_{A4}^{(0)}(p, k) = 0$. At the tree level, the three-point function satisfies

$$\Gamma_{A3}^{(0)}(p, k) = (f(p^0 + k^0) - f(k^0)) \Gamma_{R3}^{(0)}(-p, -k). \quad (55)$$

This relation is generalized to the full vertex function as

$$\Gamma_{A3}(p, k) = (f(p^0 + k^0) - f(k^0)) \Gamma_{R3}^*(-p, -k), \quad (56)$$

the proof to which is given in Appendix A.

As discussed in the previous section, $G^3(p, k)$ contains pinch singularities at weak coupling limit. Therefore, we treat $G^3(p, k)$ separately from other $G^i(p, k)$, with $i \neq 3$ in the four-point function. Suppose that $\mathcal{T}^{(A)l}_m(p, k, k')$ is the four-point function that does not include a pair of lines of the type $G^l(p, k')$. Then, the four-point function obeys the following equation:

$$\begin{aligned} \mathcal{T}_m^l(p, k, k') & = \mathcal{T}^{(A)l}_m(p, k, k') \\ & + (-i)^3 \int \frac{d^4 k''}{(2\pi)^4} \mathcal{T}^{(A)l}_n(p, k, k'') \\ & \quad \times G^n(p, k'') \mathcal{T}_m^n(p, k'', k'). \quad (57) \end{aligned}$$

In order to pick $G^3(p, k)$ up, we also define $\mathcal{T}^{(B)l}_m(p, k, k')$ as a four-point function that does not include $G^3(p + k'', k'')$. The full four-point function $\mathcal{T}^3_3(p, k, k')$ obeys the following self-consistent equation:

$$\begin{aligned} \mathcal{T}^3_3(p, k, k') & = \mathcal{T}^{(B)3}_3(p, k, k') \\ & + (-i)^3 \int \frac{d^4 k''}{(2\pi)^4} \mathcal{T}^{(B)3}_3(p, k, k'') \\ & \quad \times G^3(p, k'') \mathcal{T}^3_3(p, k'', k'). \quad (58) \end{aligned}$$

Other full four-point functions satisfy

$$\begin{aligned}
\mathcal{T}^i_j(p, k, k') &= \mathcal{T}^{(B)^i}_j(p, k, k') \\
&+ (-i)^3 \int \frac{d^4 k''}{(2\pi)^4} \mathcal{T}^{(B)^i}_3(p, k, k'') \\
&\times G^3(p, k'') \mathcal{T}^{(B)^3}_j(p, k'', k') \\
&+ (-i)^6 \int \frac{d^4 k''}{(2\pi)^4} \int \frac{d^4 k'''}{(2\pi)^4} \mathcal{T}^{(B)^i}_3(p, k', k'') \\
&\times G^3(p, k'') \mathcal{T}^3_3(p, k'', k''') \\
&\times G^3(p, k''') \mathcal{T}^{(B)^3}_3(p, k''', k'), \quad (59)
\end{aligned}$$

$$\begin{aligned}
\mathcal{T}^i_3(p, k, k') &= \mathcal{T}^{(B)^i}_3(p, k, k') \\
&+ (-i)^3 \int \frac{d^4 k''}{(2\pi)^4} \mathcal{T}^{(B)^i}_3(p, k, k'') \\
&\times G^3(p, k'') \mathcal{T}^3_3(p, k'', k'), \quad (60)
\end{aligned}$$

$$\begin{aligned}
\mathcal{T}^3_j(p, k, k') &= \mathcal{T}^{(B)^3}_j(p, k, k') \\
&+ (-i)^3 \int \frac{d^4 k''}{(2\pi)^4} \mathcal{T}^3_3(p, k, k'') \\
&\times G^3(p, k'') \mathcal{T}^{(B)^3}_3(p, k'', k'). \quad (61)
\end{aligned}$$

The diagrams corresponding to Eqs. (58)–(61) are shown in Fig. 4. Inserting Eqs. (58)–(61) into Eq. (49), we arrive at a simple form:

$$\begin{aligned}
\mathcal{G}_R^0(p) &= \frac{i}{2} \int \frac{d^4 k}{(2\pi)^4} \int \frac{d^4 k'}{(2\pi)^4} \bar{\Gamma}^*(-p, -k) (f(k^0) \\
&- f(p^0 + k^0)) G^3(p, k) [(2\pi)^4 \delta^4(k - k') \\
&+ i \mathcal{T}^3_3(p, k, k') G^3(p, k')] \bar{\Gamma}(p, k') + \mathcal{K}(p), \quad (62)
\end{aligned}$$

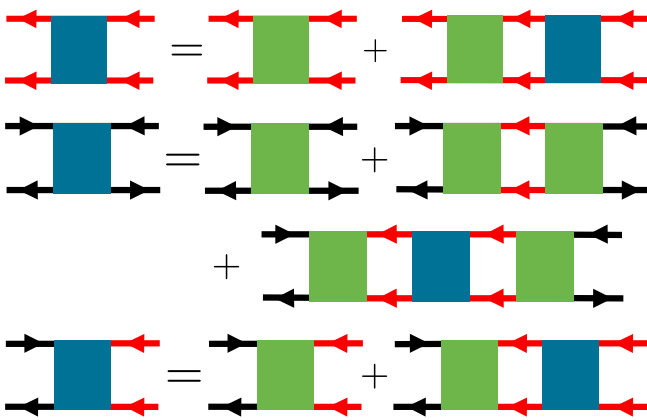


FIG. 4 (color online). Self-consistent equation for the four-point functions $\mathcal{T}^3_3(p, k, k')$, $\mathcal{T}^1_2(p, k, k')$, and $\mathcal{T}^1_3(p, k, k')$, respectively. The blue (dark gray) squares denote $\mathcal{T}^i_j(p, k, k')$, and the green (light gray) squares denote $\mathcal{T}^{(B)^i}_j(p, k, k')$.

where

$$\begin{aligned}
\mathcal{K}(p) &\equiv -\frac{i}{2} \sum_{i,j=1}^2 \int \frac{d^4 k}{(2\pi)^4} \int \frac{d^4 k'}{(2\pi)^4} \Gamma_{Ai}^{(0)}(p, k) G^i(p, k) \\
&\times [(2\pi)^4 \delta^4(k - k') \delta^i_j \\
&+ i \mathcal{T}^{(B)^i}_j(p, k, k') G^j(p, k')] \Gamma_R^{(0)j}(p, k'), \quad (63)
\end{aligned}$$

which does not include $G^3(p, k)$, so that $\mathcal{K}(p)$ is not enhanced at small p . We have also introduced the effective vertex function shown diagrammatically in Fig. 5, which is expressed as

$$\begin{aligned}
\bar{\Gamma}(p, k) &\equiv \Gamma^{(0)}(p, k) + (-i)^3 \sum_{i=1}^2 \int \frac{d^4 k'}{(2\pi)^4} \mathcal{T}^{(B)^3}_i(p, k, k') \\
&\times G^i(p, k') \Gamma_R^{(0)i}(p, k'). \quad (64)
\end{aligned}$$

This effective vertex function includes vertex corrections which can be evaluated by loop expansions, as long as further infrared singularities do not appear, and contains both quantum and medium effects; these corrections are in the same order in coupling at high temperature. We emphasize that this vertex correction is not included in the usual kinetic theory, and hence the vertex correction derived here describes an effect beyond the kinetic theory.

Now, the transport coefficient σ is given by the retarded Green function at the $p \rightarrow 0$ limit,

$$\sigma \equiv \lim_{p^0 \rightarrow 0} \lim_{p \rightarrow 0} \frac{1}{p^0} \text{Im} \mathcal{G}_R(p) \equiv \sigma_B + \sigma_{\mathcal{K}}. \quad (65)$$

Note that these limits, $p^0 \rightarrow 0$ and $p \rightarrow \mathbf{0}$, do not exchange, in general. We have decomposed the transport coefficient into two parts, $\sigma_B + \sigma_{\mathcal{K}}$, the explicit forms of which will be given shortly.

Let us discuss the two terms one-by-one. The first term is expressed as

$$\begin{aligned}
\sigma_B &\equiv \frac{1}{2} \int \frac{d^4 k}{(2\pi)^4} \int \frac{d^4 k'}{(2\pi)^4} \bar{\Gamma}^*(-k) \left(-\frac{\partial}{\partial k^0} f(k^0) \right) \\
&\times \frac{\rho(k)}{-2 \text{Im} \Pi_R(k)} \left[(2\pi)^4 \delta^4(k - k') \right. \\
&- \text{Im} \mathcal{T}^3_3(k, k') \frac{\rho(k')}{-2 \text{Im} \Pi_R(k')} \left. \right] \bar{\Gamma}(k'), \quad (66)
\end{aligned}$$

where we have used the relation

$$G^3(0, k) = D^R(k) D^A(k) = \frac{\rho(k)}{-2 \text{Im} \Pi_R(k)}, \quad (67)$$

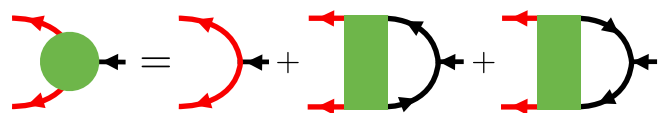


FIG. 5 (color online). Vertex corrections to $\bar{\Gamma}(p, k)$. The green squares correspond to $\mathcal{T}^{(B)^3}_i(p, k, k')$.

in accordance with Eq. (7). We have also introduced abbreviated notations:

$$\mathcal{T}^3_3(k, k') = \mathcal{T}^3_3(0, k, k'), \quad (68)$$

$$\bar{\Gamma}(k') = \bar{\Gamma}(0, k'), \quad (69)$$

$$\bar{\Gamma}^*(k) = \bar{\Gamma}^*(0, k). \quad (70)$$

The second term of the rhs in Eq. (66) is defined by

$$\sigma_{\mathcal{K}} \equiv \lim_{p^0 \rightarrow 0} \lim_{p \rightarrow 0} \frac{1}{p^0} \text{Im} \mathcal{K}(p). \quad (71)$$

As will be clarified in the next subsection, the physics content of the σ_B can be nicely given in terms of a Boltzmann equation. At the weak coupling, σ_B becomes much larger than $\sigma_{\mathcal{K}}$ because of the pinch singularity. In the following, we focus on σ_B .

Let us introduce the full vertex function, $\Gamma(k)$, by

$$\begin{aligned} \Gamma(k) &= \bar{\Gamma}(k) - \int \frac{d^4 k'}{(2\pi)^4} \text{Im} \mathcal{T}^3_3(k, k') \\ &\quad \times \frac{\rho(k')}{-2 \text{Im} \Pi_R(k')} \bar{\Gamma}(k'), \end{aligned} \quad (72)$$

which is found to obey the following self-consistent equation on account of Eq. (58):

$$\begin{aligned} \Gamma(k) &= \bar{\Gamma}(k) - \int \frac{d^4 k'}{(2\pi)^4} \text{Im} \mathcal{T}^{(B)3}_3(k, k') \\ &\quad \times \frac{\rho(k')}{-2 \text{Im} \Pi_R(k')} \Gamma(k'). \end{aligned} \quad (73)$$

The diagrammatic representation of this integral equation is given in Fig. 6.

Now, $\mathcal{T}^{(B)3}_3(p, k, k')$ consists of two parts: $\mathcal{T}^{(A)3}_3(p, k, k')$, which does not include $G^i(p, k)$, and the others. The latter part contains $\mathcal{T}^{(A)i}_3(p, k, k')$, which is proportional to $f(p^0 + k^0) - f(k^0)$, so that it vanishes as $p^0 \rightarrow 0$. Therefore, $\mathcal{T}^{(B)3}_3(k, k') = \mathcal{T}^{(A)3}_3(k, k')$. The dominant transport coefficient σ_B is now expressed as

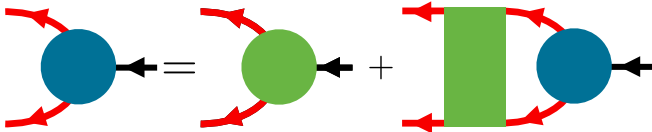


FIG. 6 (color online). The self-consistent equation for the vertex function. The blue and green blobs correspond to the full and renormalized vertex function. The green square corresponds to the collision term.

$$\sigma_B = \frac{1}{2T} \int \frac{d^4 k}{(2\pi)^4} \frac{\rho(k)}{-2 \text{Im} \Pi_R(k)} f(k^0) (1 + f(k^0)) \bar{\Gamma}^*(k) \Gamma(k), \quad (74)$$

where we have used the relation $\bar{\Gamma}^*(k) = \bar{\Gamma}^*(-k)$.

Equations (64), (73), and (74) are our main result. What we have done is rewriting diagrams in a useful and physical form. This is just a rewriting of diagrams, so that there is no approximation in the sense of the diagrammatic expansion (although nonperturbative contributions such as instantons are not included). The $\Pi_R(k)$, $\mathcal{T}^{(A)3}_3(k, k')$, and $\bar{\Gamma}(k)$ can be expanded by loops, as far as further infrared singularities appear. The spectral function is obtained through $\Pi_R(k)$. One has to choose the loop diagrams for $\Pi_R(k)$ and $\mathcal{T}^{(A)3}_3(k, k')$, so as to satisfy the symmetries of the action, i.e., the Ward-Takahashi identity, as is discussed in Appendix C 2.

Let us estimate the order of σ_B at weak coupling. The leading contribution comes from the peak of the spectral function. The residue of the pole corresponding to the peak is of order 1, and $\text{Im} \Pi_R(k)$ is of order λ^2 at the pole, so the first part in Eq. (74) gives a contribution of order $1/\lambda^2$. The four-point function, $\text{Im} \mathcal{T}^{(A)3}_3(k, k')$, in Eq. (73), is related to the squared scattering amplitude, which is of order λ^2 from $2 \rightarrow 2$ scattering. This is the same order as the imaginary part of the self-energy, so the full vertex $\Gamma(k)$ is of the same order as $\bar{\Gamma}(k)$. As we will see in the next subsection, $\text{Im} \mathcal{T}^{(A)3}_3(k, k')$ and $\text{Im} \Pi_R(k)$ are related to the collision term of a Boltzmann equation, which has the same order of the coupling constant. As a result, the σ_B is estimated as of order $1/\lambda^2$ at weak coupling. This is consistent with the result in kinetic theory where the shear viscosity is proportional to the inverse of the transport cross section of order λ^2 . We note that the σ_B diverges at the zero cutoff limit, $\kappa = 0$, for bosons, because $f(k)$ has the pole at $k^0 = 0$, while fermions do not. The divergence will be cancelled by adding $\sigma_{\mathcal{K}}$.

C. Linearized Boltzmann equation

Here, we discuss the relation between our diagrammatic method and the linearized Boltzmann equation. We will show that Eq. (73) has the form of a linearized Boltzmann equation. In the leading order of the coupling constant, it is known that the linear equation, Eq. (73), with the quasiparticle approximation is reduced to a linearized Boltzmann equation in scalar theory [13] and QED [17]. Beyond the leading order, nothing has been known about the relation between the diagrammatic method for the Kubo formula and the kinetic equation. Although the Boltzmann equation is the equation for the on-shell (quasi) particles, the spectral function includes not only the quasiparticle peak but also a multiparticle-state spectrum. If one wants to derive the Boltzmann-like equation, which contains the scattering process of the quasiparticles, one

needs to decompose the spectrum function into the quasi-particle part with a distinct peak and continuum parts for rewriting the equation in terms of the quasiparticles. In this paper, we shall not do such a decomposition; nevertheless, we shall show that the linear equation has a similar property to that of the linearized Boltzmann equation. To derive a linearized collision operator in our formalism, we define $\varphi(k)$ by

$$\varphi(k) \equiv \frac{\Gamma(k)}{-2\text{Im}\Pi_R(k)}, \quad (75)$$

following [13]. Then, Eq. (73) is cast into the following form:

$$\frac{1}{2k^0}\bar{\Gamma}(k) = \mathcal{L}\varphi(k), \quad (76)$$

where \mathcal{L} is defined by

$$\begin{aligned} \mathcal{L}\varphi(k) &\equiv -2\frac{1}{2k^0}\text{Im}\Pi_R(k)\varphi(k) + \frac{1}{2k^0} \\ &\times \int \frac{d^4k'}{(2\pi)^4}\rho(k')\text{Im}\mathcal{T}^{(A)3}_3(k, k')\varphi(k'). \end{aligned} \quad (77)$$

We note that $\varphi(k)$ is an odd (even) function under $k \leftrightarrow -k$, if $\Gamma(k)$ is an even (odd) function, since $\text{Im}\Pi_R(k)$ is an odd function. Equation (76) has the same form as the linearized Boltzmann equation [29]. In fact, \mathcal{L} can be identified with the linearized collision operator: The equivalence between Eq. (76) and the linearized Boltzmann equation in the leading order of the coupling constant is shown in Appendix B.

Here, we introduce an inner product as

$$\langle \varphi_1, \varphi_2 \rangle \equiv \int \frac{d^4k}{(2\pi)^4} W(k)\varphi_1^*(k)\varphi_2(k), \quad (78)$$

where $W(k) \equiv k^0(1 + f(k^0))f(k^0)\rho(k) > 0$ is the weight function, and φ_1 and φ_2 are arbitrary functions of k^μ . We note that $W(k)$ at $k_0 = 0$ is finite, although $f(k^0)$ has a singularity at $k_0 = 0$. Using this inner product, we can rewrite the transport coefficient, Eq. (74), as

$$\sigma_B = \frac{1}{T}\langle \mathcal{S}, \mathcal{L}^{-1}\mathcal{S} \rangle, \quad (79)$$

where $\mathcal{S} \equiv \bar{\Gamma}/(2k^0)$. Note that \mathcal{S} must be orthogonal to the eigenvectors of \mathcal{L} with zero eigenvalues corresponding to conserved charges; otherwise, \mathcal{L}^{-1} is not well-defined.

The inverse of the collision operator can be expressed as

$$\mathcal{L}^{-1} = \int_0^\infty dt e^{-t\mathcal{L}}, \quad (80)$$

where we have assumed that the eigenvalues of \mathcal{L} are nonnegative. This is necessary for the stability of the system. Using Eq. (80), Eq. (79) is rewritten as a Kubo formula for the quasiparticle

$$\sigma_B = \frac{1}{T} \int_0^\infty dt \langle \mathcal{S}(0), \mathcal{S}(t) \rangle, \quad (81)$$

where $\mathcal{S}(t) = \exp(-t\mathcal{L})\mathcal{S}(0)$. We rewrite a Kubo formula in field theory to that for relevant quasiparticles. Equation (81) is a semiclassical formula, i.e., no field operator is present in Eq. (81). The collision operator and the effective vertex are calculated in thermal field theory. We note that the thermal weight $W(k)$ does not contain $f(k^0)$ but $f(k^0)(1 + f(k^0))$, because the thermal average is taken for a two-point correlation function. If the \mathcal{S} is an eigenstate of \mathcal{L} with an eigenvalue $1/\tau$,

$$\sigma_B = \frac{\tau}{T} \langle \mathcal{S}(0), \mathcal{S}(0) \rangle. \quad (82)$$

The inverse of the eigenvalue τ can be identified as a relaxation time.

Let us estimate the shear viscosity using Eq. (82) in the quasiparticle limit, where the thermal weight function becomes

$$W(k) \simeq 2\pi[\delta(k^0 - |\mathbf{k}|) + \delta(k^0 + |\mathbf{k}|)]f(|\mathbf{k}|)(1 + f(|\mathbf{k}|)), \quad (83)$$

and the vertex function for the shear viscosity π^{ij} in the leading order is

$$\pi^{ij} = \frac{1}{k^0} \left(k^i k^j - \delta^{ij} \frac{\mathbf{k}^2}{3} \right). \quad (84)$$

Then, the shear viscosity is evaluated as

$$\eta = \frac{\tau}{10T} \langle \pi^{ij}, \pi_{ij} \rangle = \frac{\tau s T}{5}, \quad (85)$$

where $s = 2\pi^2 T^3/45$ is the entropy density in the free theory. Using $P = 4s$ for free massless particles in the leading order, we obtain the relaxation time as

$$\tau = \frac{5}{4} \frac{\eta}{P}. \quad (86)$$

This is 25% larger than that obtained in Ref. [30], although Eq. (85) is a parametrically similar equation to that given in Ref. [30]. The difference comes from the semiclassical calculation in our formalism and the field theoretical calculation in Ref. [30].

D. Leading and higher orders

In this subsection, we show how the contributions of the higher- as well as leading-order terms to the transport coefficient appear in our formalism. The transport coefficient σ_B in Eq. (79) consists of the vertex function \mathcal{S} , the collision term \mathcal{L} , and the inner product that contains the spectral function $\rho(k)$. The contribution of the leading- and higher-order terms is nicely summarized into these terms. The merit of our formalism is that the contributions of each term can be systematically estimated using loop expansions. To show the details of this statement, let us consider the shear viscosity as an example. We will find the shear viscosity is expanded by the coupling constant λ as

$$\frac{\eta}{\eta_0} = 1 + c_1\sqrt{\lambda} + (c_2' \ln 1/\lambda + c_2)\lambda + \dots \quad (87)$$

Here, the numerical calculation in the leading order gives $\eta_0 \simeq 3033.54T^3/\lambda^2$ [13,22].

First, let us begin with clarifying how the λ^{-2} dependence of η_0 is obtained in the leading order within our formalism, although a brief discussion on this matter was given in the end of Subsec. IV B. The diagram of $\mathcal{T}^{(A)3}_3(k, k')$ in the leading order is shown in Fig. 7, which corresponds to the $2 \rightarrow 2$ scattering. Then, the squared scattering amplitude is proportional to λ^2 , and thus the collision term is estimated as $\mathcal{L} \sim \mathcal{T}^{(A)3}_3(k, k') \sim \lambda^2$. In this calculation, the quasiparticle approximation with a vanishing mass is employed in the spectral function, $\rho(k) = (2\pi)\text{sgn}(k^0)\delta(k^2)$, because hard momenta of order $k \sim T$ contribute to the leading order, where the mass can be neglected. Formally, the diagram in the left-hand side of Fig. 7 also contains $1 \rightarrow 3$ decay and $3 \rightarrow 1$ fusion processes; however, they are found to be higher orders of the coupling because of the phase space restricted by the energy-momentum conservation. The contribution of \mathcal{S} is of order one. As a result, we have $\eta_0 \sim \mathcal{S}^2/\mathcal{L} \sim 1/\lambda^2$, which coincides with the result given by the Boltzmann equation. In fact, the equivalence between the diagrammatic method in the leading order and the linearized Boltzmann equation generally holds, as is proven in Appendix B.

Next, let us estimate the contribution of the next leading order (NLO) to the shear viscosity in Eq. (87), in which contributions are found to come from the correction to $\rho(k)$, while the loop corrections to \mathcal{S} and \mathcal{L} , at least of order λ , are higher-order corrections. The spectral functions are characterized by the thermal mass, width, and height of the peak of the quasiparticle. In the NLO, the thermal-mass correction gives the contribution of order $\sqrt{\lambda}$, which is nonanalytic in λ [22]. The nonanalytic term is obtained from a phase space integral with an infrared enhancement of the Bose-Einstein distribution function $f(E) \simeq T/E$ at small E . Since $\rho(k)$ appears with $f(k)$ in \mathcal{L} , \mathcal{S} , and the inner product [see, e.g., Eq. (B11)], consider the following integral to see the nonanalyticity of λ :

$$\int \frac{d^4p}{(2\pi)^4} \rho(p) f(p) = \frac{T^2}{12} \left[1 + a_1 \frac{m_T}{2\pi T} + \left(a_2' \ln \left(\frac{m_T}{2\pi T} \right)^2 + a_2 \right) \times \left(\frac{m_T}{2\pi T} \right)^2 + \dots \right], \quad (88)$$

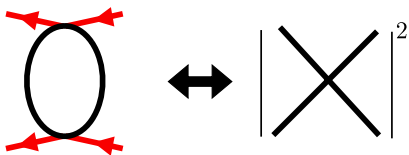


FIG. 7 (color online). The diagram contributing to $\mathcal{T}^{(A)3}_3(k, k')$ in the leading order, which corresponds to $2 \rightarrow 2$ scattering.

where $a_1 = 6$, $a_2 = 3 - 6\gamma_E + 6\ln 2$, and $a_2' = 3$, with the Euler constant $\gamma_E = 0.577216$. We have assumed that the spectral function has a form $\rho(k) = (2\pi)\text{sgn}(k^0)\delta(k^2 - m_T^2)$ to obtain Eq. (88). The nonanalytic term m_T appears in the rhs of Eq. (88), although the integrand is a function of m_T^2 , which is obtained as [31]

$$m_T^2 = \frac{\lambda T^2}{24} \left[1 - 3 \left(\frac{\lambda}{24\pi^2} \right)^{(1/2)} + \dots \right]. \quad (89)$$

The thermal masses in the leading ($\sim \lambda$) and the next leading ($\sim \lambda^{3/2}$) orders are given by the one-loop diagram and the ring diagram resummation, respectively. Therefore, the contribution of the phase space integral in the NLO gives that of order $\sqrt{\lambda}$, and the coefficient is estimated as $c_1 \simeq 0.104$ [22]. We note that this term also contains the next-to-next-leading-order (NNLO) corrections of orders $\lambda \ln 1/\lambda$ and λ to the shear viscosity from Eqs. (88) and (89). One might worry about corrections from the thermal width of the spectral function; however, this is in even higher orders because the width is of order $\lambda^2 T$, which is smaller than λT .

Finally, we identify diagrams contributing to the shear viscosity in the NNLO corrections. To our knowledge, this is the first identification of the diagrams contributing to the NNLO corrections. As noted above, the thermal-mass correction to $\rho(k)$ is one of them. The corrections in the NLO to \mathcal{S} and \mathcal{L} can generally contribute to the transport coefficient in the NNLO. However, for the shear viscosity, the correction to \mathcal{S} does not contribute in the NNLO. The reason is as follows: The diagrams which contribute to the vertex corrections of up to order λ^2 are shown in Fig. 8. The second and third diagrams corresponding to the NLO corrections to \mathcal{S} are ring diagrams, which do not depend on the external momentum k . However, the contributions of the ring diagrams vanish because the vertex function \mathcal{S} for the shear viscosity is a second rank tensor and proportional to $k^i k^j - \delta^{ij} k^2$. Thus, the corrections to \mathcal{S} start from those of order λ^2 that are higher orders of the coupling. The diagrams of the leading-order and NLO corrections to $\mathcal{T}^{(A)3}_3(k, k')$ are shown in Fig. 9. These corrections correspond to quantum and thermal loop corrections of order λ^3 to the squared scattering amplitude of the $2 \rightarrow 2$ process, which do not include multiple scattering such as $3 \rightarrow 3$ and $2 \rightarrow 4$. A typical diagram corresponding to the $3 \rightarrow 3$ process is shown in Fig. 10, whose process contributes to the next-to-next-to-next leading order, since the squared amplitude is proportional to λ^4 . In summary of the NNLO correction to the shear viscosity, the corrections of the

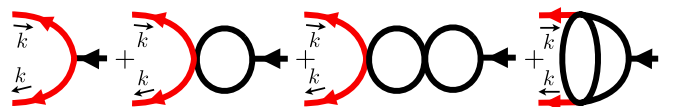


FIG. 8 (color online). Vertex corrections up to of order λ^2 .

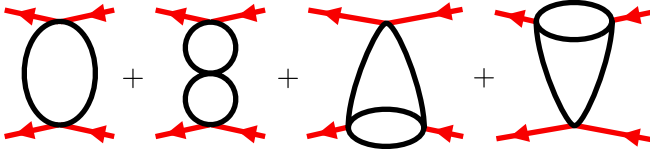


FIG. 9 (color online). Diagrams of order λ^3 contributing to $\mathcal{T}^{(A)3}_3(k, k')$.

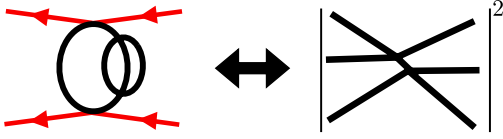


FIG. 10 (color online). Collision term at the leading order corresponding to $3 \rightarrow 3$ scattering.

thermal mass of up to order $\lambda^{3/2}$ and the squared scattering amplitude of order λ^3 contribute to the NNLO, while the corrections to \mathcal{S} do not.

V. CONCLUSION AND OUTLOOK

We have given a formulation of a resummation method for computing transport coefficients in relativistic quantum field theory, using the ϕ^4 theory as an example. We separated the diagrams in the dominant part from the other diagrams and reformulated them in a way which makes the included physics instructive, by adapting the Eliashberg method to a relativistic case in the real-time formalism. Our results are summarized in Eqs. (64), (73), and (74). The self-consistent equation of the vertex, Eq. (73), has the meaning of a kinetic equation, and has a form similar to the linearized Boltzmann equation. In the leading order of the coupling constant, we recover the kinetic equation of previous works [13] (see Appendix B). The higher-order corrections beyond the leading order are systematically incorporated in the formalism for the first time and found to be nicely summarized as the renormalization of the vertex correction, Eq. (64); the spectral function, $\rho(k)$; and the collision term through $\text{Im}\mathcal{T}^{(A)3}_3(k, k')$ and $\text{Im}\Pi_R(k)$. In the higher orders of the collision term, both effects of multiple scattering and quantum loops are expressed in a power of the coupling constant. Their effects also appear in the vertex correction. The higher-order correction is important to see the convergence of the perturbation theory at finite temperature.

We have identified the diagrams up to the next-to-next-leading-order corrections in the weak coupling expansion of ϕ^4 theory. The detailed calculation for the higher-order corrections will be discussed in our future work [32]. We emphasize that the advantage of our diagrammatic method is to enable us to identify diagrams contributing to the higher-order corrections, which is a difficult task in kinetic approaches and other diagrammatic methods.

Although the formalism is developed using the ϕ^4 theory in the present work, the generalization of it to fermionic theories is straightforward: The Bose-Einstein distribution function in the self-consistent equation is simply replaced by the Fermi-Dirac distribution function. The spinor structure is introduced into the vertex function and the collision term. Since the Fermi-Dirac distribution function $n_F(E)$ does not diverge at $E = 0$, the infrared cutoff introduced in Sec. IV A is not necessary.

Gauge theory is more complicated. Resummation of collinear divergences, in addition to the ladder diagrams, is necessary to obtain the correct result in certain orders of the coupling constant, which is called the Landau-Pomeranchuk-Migdal effect [33]. The self-consistent equation summing the collinear singularities over has the form of the Boltzmann equation with the collision term in $1 \rightarrow 2$ and $2 \rightarrow 1$ processes [17,20,34].

It is also interesting to apply the diagram method to critical phenomena, where the hydrodynamic mode and the fluctuation of the order parameter play an important role. We have to take into account these modes in addition to quasiparticle modes.

ACKNOWLEDGMENTS

This work was partially supported by a Grant-in-Aid for Scientific Research by the Ministry of Education, Culture, Sports, Science, and Technology (MEXT) of Japan (No. 20540265 and No. 19.07797), by the Yukawa International Program for Quark-Hadron Sciences, and by the Grant-in-Aid for the global COE program ‘‘The Next Generation of Physics, Spun from Universality and Emergence’’ from MEXT.

APPENDIX A: SEVERAL IDENTITIES IN THE REAL-TIME FORMALISM

In this Appendix, we show several useful identities in the R/A basis [27]. We start with the standard basis. The largest and smallest time equation shows

$$\sum_{\{i_k\}} \Gamma_{i_1 i_2 \dots i_n}(p_1, p_2, \dots, p_n) \prod_{i_k=2} e^{-\sigma p_k^0} = 0, \quad (\text{A1})$$

and the Kubo-Martin-Schwinger relation shows

$$\sum_{\{i_k\}} \Gamma_{i_1 i_2 \dots i_n}(p_1, p_2, \dots, p_n) \prod_{i_k=2} e^{(\beta-\sigma)p_k^0} = 0. \quad (\text{A2})$$

By diagrammatic analysis, one finds [27]

$$\begin{aligned} & \Gamma_{i_1 i_2 \dots i_n}^*(p_1, p_2, \dots, p_n) \\ &= -\Gamma_{\bar{i}_1 \bar{i}_2 \dots \bar{i}_n}(p_1, p_2, \dots, p_n) \prod_{i_k=2} e^{-(\beta-2\sigma)p_k^0}. \end{aligned} \quad (\text{A3})$$

Equations (A1)–(A3) are basic identities in the real-time formalism [35]. In the R/A basis, Eq. (A1) becomes

$$\begin{aligned}
& \sum_{\{i_k\}} \prod_{m=1}^n U^{\alpha_m}_{i_m}(p_m) \prod_{i_k=2} e^{-\sigma p_k^0} \Gamma_{\alpha_1 \alpha_2 \dots \alpha_n}(p_1, p_2, \dots, p_n) \\
&= \prod_{m=1}^n [U^{\alpha_m}_1(p_m) + U^{\alpha_m}_2(p_m) e^{-\sigma p_m^0}] \\
&\quad \times \Gamma_{\alpha_1 \alpha_2 \dots \alpha_n}(p_1, p_2, \dots, p_n) \\
&= \Gamma_{RR \dots R}(p_1, p_2, \dots, p_n) \prod_{m=1}^n (e^{\beta p_m^0} - 1) = 0. \quad (\text{A4})
\end{aligned}$$

Since $e^{\beta p_m^0} - 1 \neq 0$,

$$\Gamma_{RR \dots R}(p_1, p_2, \dots, p_n) = 0. \quad (\text{A5})$$

Similarly, Eq. (A2) becomes, in this basis,

$$\Gamma_{AA \dots A}(p_1, p_2, \dots, p_n) = 0. \quad (\text{A6})$$

Therefore, the vertex function vanishes when all indices are the same. This means particles are neither produced from the thermal equilibrium system nor absorbed into the system, similar to the vacuum at zero temperature and zero density.

Equation (A3) is reduced to

$$\begin{aligned}
& \Gamma_{\alpha_1 \alpha_2 \dots \alpha_n}^*(p_1, p_2, \dots, p_n) \\
&= \Gamma_{i_1 i_2 \dots i_n}^*(p_1, p_2, \dots, p_n) \prod_{m=1}^n U^{i_m}_{\alpha_m}(p_m) \\
&= -\Gamma_{\bar{\alpha}_1 \bar{\alpha}_2 \dots \bar{\alpha}_n}(p_1, p_2, \dots, p_n) \prod_{\alpha_m=R} f(p_m^0) \prod_{\alpha_m=A} \frac{1}{-f(-p_m^0)}. \quad (\text{A7})
\end{aligned}$$

For a two-point function,

$$\Gamma_{AR}^*(-k, k) = \Gamma_{RA}(-k, k), \quad (\text{A8})$$

implying $D^R(k) = D^A(k)$. For a three-point function,

$$\Gamma_{RAA}^*(p, q, k) = -\Gamma_{ARR}(p, q, k) \frac{1}{f(p+k) - f(k)}. \quad (\text{A9})$$

Therefore,

$$-(f(p+k) - f(k)) \Gamma_{RAA}^*(p, q, k) = \Gamma_{ARR}(p, q, k). \quad (\text{A10})$$

For a four-point function,

$$\begin{aligned}
\mathcal{T}_{AARR}^*(p_1, p_2, p_3, p_4) &= -\mathcal{T}_{RRAA}(p_1, p_2, p_3, p_4) \\
&\quad \times \frac{f(p_3^0) f(p_4^0)}{f(-p_1^0) f(-p_2^0)}. \quad (\text{A11})
\end{aligned}$$

APPENDIX B: RELATION BETWEEN BOLTZMANN EQUATION AND KUBO FORMULA IN THE LEADING ORDER

Here, we explicitly show that Eq. (77) is equivalent to a linearized Boltzmann equation in the leading order. This was shown in Ref. [13] in a different formalism. Let us start with a Boltzmann equation,

$$2k^\mu \partial_\mu f(x, k) = -C[f], \quad (\text{B1})$$

where $f(x, k)$ denotes the distribution function, and $C[f]$ is the collision term. In the leading order, the collision term has the form of a $2 \rightarrow 2$ collision,

$$\begin{aligned}
C[f] &= \frac{1}{2} \int \frac{d^3 k'}{(2\pi)^3} \frac{1}{2E_{k'}} \int \frac{d^3 q}{(2\pi)^3} \frac{1}{2E_q} \int \frac{d^3 q'}{(2\pi)^3} \frac{1}{2E_{q'}} \\
&\quad \times |\mathcal{M}|^2 (2\pi)^4 \delta^{(4)}(k + q - k' - q') \\
&\quad \times [f_k f_q (1 + f_{k'}) (1 + f_{q'}) \\
&\quad - (1 + f_k) (1 + f_q) f_{k'} f_{q'}], \quad (\text{B2})
\end{aligned}$$

where \mathcal{M} is the scattering amplitude, and $\mathcal{M} = i\lambda$ for ϕ^4 theory in the leading order. At (local) thermal equilibrium, the distribution function has the form

$$f_0(x, k) = \frac{1}{\exp(\beta(x) u_\mu(x) k^\mu) - 1}, \quad (\text{B3})$$

where $u_\mu(x)$ is the local velocity, k^μ is the four-momentum at on shell, and $k^2 = m^2$ with mass m . Here, we consider the shear flow; then, the left-hand side of Eq. (B1) becomes

$$2k^\mu \partial_\mu f_0(x, p) = -\beta f_0(x, p) (1 + f_0(x, p)) \Gamma^{ij}(k) \frac{1}{2} \sigma_{ij}(x), \quad (\text{B4})$$

where $\Gamma^{ij}(k) = 2k^i k^j - 2\delta^{ij} k^2/3$, and

$$\sigma_{ij} = \partial_i u_j(x) + \partial_j u_i(x) - \frac{2}{3} \delta_{ij} \partial_k u_k. \quad (\text{B5})$$

We have considered the local rest frame, $u_\mu = (1, \mathbf{0})$. Note that, at the local rest frame, $\partial_i u_j(x)$ is nonzero, although $u_i(x) = 0$. By linearizing the Boltzmann equation around the thermal equilibrium $f(x, k) = f_0(x, k) + \delta f(x, k)$, one finds

$$\begin{aligned}
C[f] &\simeq \beta (1 + f_0(E_k)) \frac{\lambda^2}{2} \int \frac{d^3 k_q}{(2\pi)^3} \frac{1}{2E_q} (1 + f_0(E_q)) \\
&\quad \times \int \frac{d^3 k'}{(2\pi)^3} \frac{1}{2E_{k'}} f_0(E_{k'}) \int \frac{d^3 k_{q'}}{(2\pi)^3} \frac{1}{2E_{q'}} f_0(E_{q'}) \\
&\quad \times (2\pi)^4 \delta^{(4)}(k + q - k' - q') \\
&\quad \times [\varphi^{ij}(k) + \varphi^{ij}(q) - \varphi^{ij}(k') - \varphi^{ij}(q')] \frac{1}{2} \sigma_{ij} \\
&\equiv 2E_k \beta f_0(E_k) (1 + f_0(E_k)) \mathcal{L}_{\text{Boltz}} \varphi^{ij} \frac{1}{2} \sigma_{ij}, \quad (\text{B6})
\end{aligned}$$

where $f_0(E_q) \equiv f_0(x, k)$ at the local rest frame, $\mathcal{L}_{\text{Boltz}}$ is the linearized collision operator, and we choose $\delta f(x, k) = \beta f_0(E_k)(1 + f_0(E_k))\varphi^{ij}(k)\sigma_{ij}/2$. Then, the linearized equation reads

$$\frac{\Gamma^{ij}(k)}{2E_k} = \mathcal{L}_{\text{Boltz}}\varphi^{ij}(k). \quad (\text{B7})$$

This is the same form as Eq. (76). Let us check $\mathcal{L} = \mathcal{L}_{\text{Boltz}}$ at weak coupling. For this purpose, let us estimate the four-point function, $\text{Im}\mathcal{T}^{(A)3}_3(k, k')$, and $\text{Im}\Pi_R^{\text{two-loop}}(k)$. Using the Feynman rule, Eqs. (28)–(36), we find

$$\begin{aligned} \text{Im}\mathcal{T}^{(A)3}_3(k, k') &= -\frac{1}{2}\lambda^2(e^{\beta k^0} - 1)f(k'^0) \int \frac{d^4q}{(2\pi)^4}(1 + f(q^0))\rho(q) \\ &\quad \times \int \frac{d^4q'}{(2\pi)^4}f(q'^0)\rho(q')(2\pi)^4\delta(k + q - k' - q'), \end{aligned} \quad (\text{B8})$$

and

$$\begin{aligned} \text{Im}\Pi_R^{\text{two-loop}}(k) &= -(e^{\beta k^0} - 1)\frac{\lambda^2}{12} \int \frac{d^4q}{(2\pi)^4}(1 + f(q^0))\rho(q) \\ &\quad \times \int \frac{d^4q'}{(2\pi)^4}f(q'^0)\rho(q') \int \frac{d^4k'}{(2\pi)^4}f(k'^0)\rho(k') \\ &\quad \times (2\pi)^4\delta^{(4)}(k + q - k' - q'). \end{aligned} \quad (\text{B9})$$

Comparing Eqs. (B8) and (B9), we find

$$\text{Im}\Pi_R^{\text{two-loop}}(k) = \frac{1}{6} \int \frac{d^4k'}{(2\pi)^4}\rho(k') \text{Im}\mathcal{T}^{(A)3}_3(k, k'). \quad (\text{B10})$$

The collision term becomes

$$\begin{aligned} \mathcal{L}\varphi^{ij}(k) &= -2\frac{1}{2k^0} \text{Im}\Pi_R^{\text{two-loop}}(k)\varphi^{ij}(k) + \frac{1}{2k^0} \int \frac{d^4k'}{(2\pi)^4}\rho(k') \text{Im}\mathcal{T}^{(A)3}_3(k, k')\varphi^{ij}(k') \\ &= \frac{f^{-1}(k^0)}{2k^0} \frac{\lambda^2}{6} \int \frac{d^4k'}{(2\pi)^4}f(k'^0)\rho(k') \int \frac{d^4q}{(2\pi)^4}(1 + f(q^0))\rho(q) \\ &\quad \times \int \frac{d^4q'}{(2\pi)^4}f(q'^0)\rho(q')(2\pi)^4\delta^{(4)}(k + q - k' - q')[\varphi^{ij}(k) - \varphi^{ij}(k') + \varphi^{ij}(q) - \varphi^{ij}(q')]. \end{aligned} \quad (\text{B11})$$

Here, we have used the relation $\varphi^{ij}(-k) = -\varphi^{ij}(k)$, derived from Eq. (75), to obtain the third line. Equation (B11) includes positive and negative energies, while Eq. (B6) includes only the positive energy. This collision term contains three processes: $1 \rightarrow 3$, $2 \rightarrow 2$, and $3 \rightarrow 1$ scatterings. $1 \rightarrow 3$ and $3 \rightarrow 1$ collisions can be neglected in the leading order because the on-shell condition of quasiparticle does not satisfy. Then, the collision term for the positive energy state, $k^0 > 0$, becomes

$$\begin{aligned} \mathcal{L}\varphi^{ij}(k) &= \frac{f^{-1}(k^0)}{2k^0} \frac{\lambda^2}{2} \int \frac{d^4k'}{(2\pi)^4}f(k'^0)\rho(k')\theta(k'^0) \\ &\quad \times \int \frac{d^4q}{(2\pi)^4}(1 + f(q^0))\rho(q)\theta(q^0) \\ &\quad \times \int \frac{d^4q'}{(2\pi)^4}f(q'^0)\rho(q')\theta(q'^0)(2\pi)^4 \\ &\quad \times \delta^{(4)}(k + q - k' - q') \\ &\quad \times [\varphi^{ij}(k) - \varphi^{ij}(k') + \varphi^{ij}(q) - \varphi^{ij}(q')]. \end{aligned} \quad (\text{B12})$$

By using the quasiparticle approximation,

$$\rho(k)\theta(k^0) = \frac{1}{2E_k}(2\pi)\delta(k^0 - E_k), \quad (\text{B13})$$

with $E_k = \sqrt{k^2 + m_T^2}$, we obtain the collision operator as

$$\begin{aligned} \mathcal{L}\varphi^{ij}(k) &= \frac{f^{-1}(E_k)}{2E_k} \frac{\lambda^2}{2} \int \frac{d^3k'}{(2\pi)^3} \frac{1}{2E_{k'}}f(E_{k'}) \\ &\quad \times \int \frac{d^3q}{(2\pi)^3} \frac{1}{2E_q}(1 + f(E_q)) \\ &\quad \times \int \frac{d^3q'}{(2\pi)^3} \frac{1}{2E_{q'}}f(E_{q'})(2\pi)^4\delta^{(4)}(k + q - k' - q') \\ &\quad \times [\varphi^{ij}(k) - \varphi^{ij}(k') + \varphi^{ij}(q) - \varphi^{ij}(q')]. \end{aligned} \quad (\text{B14})$$

Thus, the collision operator in the Boltzmann equation is equivalent to that in the diagrammatic method in the leading order, $\mathcal{L} = \mathcal{L}_{\text{Boltz}}$. In the neutral scalar theory, the negative energy state is identical to the positive energy state, so that the collision term for the negative energy state is the same as that for the positive energy state.

APPENDIX C: SOME PROPERTIES OF THE COLLISION OPERATOR

The collision operator of the linearized Boltzmann equation has some basic properties: semipositive definiteness, self-adjointness, and the conserved charges being the collision invariants. Here, we focus on the self-adjointness and the conserved charges being the collision invariants,

although the semipositive definiteness of the collision operator is necessary to ensure the stability of the thermal equilibrium.

1. Self-adjointness of the collision operator

In order to show the self-adjointness, we write the linearized collision operator as

$$\mathcal{L} \varphi(k) = \int \frac{d^4 k'}{(2\pi)^4} W(k') \mathcal{L}(k, k') \varphi(k'), \quad (\text{C1})$$

where

$$\begin{aligned} \mathcal{L}(k, k') &= \frac{-1}{k^0} \text{Im} \Pi_R(k) W^{-1}(k') \delta(k - k') \\ &+ \frac{1}{2k^0} \text{Im} \mathcal{T}^{(A)^3}_3(k, k') W^{-1}(k') \rho(k'). \end{aligned} \quad (\text{C2})$$

This is the momentum representation of the linearized collision operator. The Hermitian conjugate is defined as

$$\langle \varphi_1, \mathcal{L} \varphi_2 \rangle = \langle \mathcal{L}^\dagger \varphi_1, \varphi_2 \rangle, \quad (\text{C3})$$

which means that

$$\begin{aligned} \langle \varphi_1, \mathcal{L} \varphi_2 \rangle &= \int \frac{d^4 k}{(2\pi)^4} W(k) \varphi_1^*(k) \\ &\times \left[\int \frac{d^4 k'}{(2\pi)^4} W(k') \mathcal{L}(k, k') \varphi_2(k') \right] \\ &= \int \frac{d^4 k'}{(2\pi)^4} W(k') \\ &\times \left[\int \frac{d^4 k}{(2\pi)^4} W(k) \mathcal{L}^*(k, k') \varphi_1(k) \right]^* \varphi_2(k'), \end{aligned} \quad (\text{C4})$$

$$\begin{aligned} \langle \mathcal{L}^\dagger \varphi_1, \varphi_2 \rangle &= \int \frac{d^4 k'}{(2\pi)^4} W(k') \\ &\times \left[\int \frac{d^4 k}{(2\pi)^4} W(k) \mathcal{L}^\dagger(k', k) \varphi_1(k) \right]^* \varphi_2(k'), \end{aligned} \quad (\text{C5})$$

or

$$\mathcal{L}^\dagger(k', k) = \mathcal{L}^*(k, k'). \quad (\text{C6})$$

Let us check the self-adjointness or Hermiticity, $\mathcal{L}^\dagger = \mathcal{L}$. The first term of the rhs in Eq. (C2) is obviously symmetric under $k \leftrightarrow k'$. The four-point function, $\mathcal{T}^{(A)^3}_3(k, k')$, in Eq. (C2) has a symmetry,

$$\mathcal{T}^{(A)^3}_3(k, k') = -\mathcal{T}^{(A)^3}_3(k', k) \frac{f(k')(1 + f(k'))}{f(k)(1 + f(k))}, \quad (\text{C7})$$

from Eq. (A11). Thus, the second term of the rhs in Eq. (C2) is symmetric:

$$\begin{aligned} \text{Im} \mathcal{T}^{(A)^3}_3(k, k') f^{-1}(k^0) (1 + f(k^0))^{-1} \\ = \text{Im} \mathcal{T}^{(A)^3}_3(k', k) f^{-1}(k^0) (1 + f(k^0))^{-1}. \end{aligned} \quad (\text{C8})$$

Therefore, the collision operator is Hermitian, $\mathcal{L}^\dagger = \mathcal{L}$. More precisely, the collision operator is symmetric because Eq. (C2) is a real function.

2. Collision invariant and Ward-Takahashi identity

In this subsection, we derive the Ward-Takahashi (WT) identity in the R/A basis and show that the WT identity implies that the conserved charges are zero modes of the collision operator, Eq. (77). In the imaginary-time formalism, the WT identity is derived in Refs. [17,36,37]. The WT identity is useful to constrain diagrams in order to keep symmetries in the resummed perturbation theory [17]. Conversely, to obtain the correct result in a certain order of perturbation theory, the collision term must satisfy the WT identity.

The conserved current in ϕ^4 theory is an energy-momentum current, defined by

$$j_\nu^\mu = T_\nu^\mu = \partial_\nu \phi \partial^\mu \phi - \delta_\nu^\mu \mathcal{L}. \quad (\text{C9})$$

In particular, the charge density of the momentum current is the bilinear operator,

$$j_i^0 = \partial_i \phi \partial^0 \phi. \quad (\text{C10})$$

This bilinear form is important to relate the WT identity and collision term, as we will see later. In order to derive the WT identity in a thermal bath, consider the following correlation function:

$$\langle T_C j_i^\mu(z) \phi(x) \phi(y) \rangle, \quad (\text{C11})$$

where T_C denotes a complex-time-path ordering, shown in Fig. 1. Taking $\partial_{z\mu}$, we obtain

$$\begin{aligned} \partial_{z\mu} \langle T_C j_i^\mu(z) \phi(x) \phi(y) \rangle \\ = \delta_C(z^0 - x^0) \langle T_C [j_i^0(z), \phi(x)] \phi(y) \rangle \\ + \delta_C(z^0 - y^0) \langle T_C \phi(x) [j_i^0(z), \phi(y)] \rangle, \end{aligned} \quad (\text{C12})$$

where we used the conservation law $\partial_\mu j_i^\mu = 0$. Noting that the equal-time commutation relation gives an infinitesimal translation,

$$[j_i^0(z), \phi(x)] = -i\delta^{(3)}(z - x) \partial_i \phi(x), \quad (\text{C13})$$

we obtain

$$\begin{aligned} \partial_{z\mu} \langle T_C j_i^\mu(z) \phi(x) \phi(y) \rangle &= -i\delta_C^{(4)}(z - x) \langle T_C \partial_i \phi(x) \phi(y) \rangle \\ &- i\delta_C^{(4)}(z - y) \langle T_C \phi(x) \partial_i \phi(y) \rangle. \end{aligned} \quad (\text{C14})$$

This is the WT identity in the coordinate space on the complex-time path. In the real-time formalism, the complex path is decomposed into four parts, as shown in Fig. 1. In the standard basis, Eq. (C14) becomes

$$\begin{aligned}
& \partial_{z\mu} \langle T_C j_{i;c}^\mu(z) \phi^a(x) \phi^b(y) \rangle \\
&= -iX_{cd}^a \delta^{(4)}(z-x) \langle T \partial_{zi} \phi^d(z) \phi^b(y) \rangle \\
&\quad - iX_c^b \delta^{(4)}(z-y) \langle T \phi^a(x) \partial_{zi} \phi^d(z) \rangle, \quad (C15)
\end{aligned}$$

where $j_{i;c}^0(x) = X_{cde} \partial_i \phi^d(x) \partial^0 \phi^e(x)$ with $X_{cde} = \delta_{cd} g_{de}$. Using the propagator and the three-point vertex $\Gamma^\mu(z, w, w')$, we obtain

$$\begin{aligned}
& \partial_{z\mu} \int d^4w \int d^4w' \Gamma_{i;cde}^\mu(z, w, w') D^{da}(w, x) D^{eb}(w', y) \\
&= -iX_{cd}^a \delta^{(4)}(z-x) \partial_{zi} D^{db}(z, y) \\
&\quad - iX_c^b \delta^{(4)}(z-y) \partial_{zi} D^{da}(z, x). \quad (C16)
\end{aligned}$$

In momentum space, this becomes

$$\begin{aligned}
& ip_\mu \Gamma_{i;cde}^\mu(p, q, k) D^{da}(q) D^{eb}(k) \\
&= -k_i X_{cd}^a D^{db}(k) - q_i X_c^b D^{da}(q), \quad (C17)
\end{aligned}$$

where p, k , and q are not independent but satisfy $p + k + q = 0$. Multiplying both sides of Eq. (C17) by $D_{aa'}^{-1}(q) D_{bb'}^{-1}(k)$, we find

$$ip_\mu \Gamma_{i;ca'b'}^\mu(p, q, k) = -k_i X_{cb'}^d D_{da'}^{-1}(q) - q_i X_c^d D_{db'}^{-1}(k). \quad (C18)$$

At tree level, this is reduced to

$$ip_\mu \Gamma_{(0)i;cab}^\mu(p, q, k) = -k_i X_{cb}^d D_{F,da}^{-1}(q) - q_i X_c^d D_{F,cb}^{-1}(k), \quad (C19)$$

where $\Gamma_{(0)i;cab}^\mu(p, q, k)$ is the tree-level vertex,

$$\Gamma_{(0)i;cab}^\mu(p, q, k) = X_{cab} (- (q_i k^\mu + k_i q^\mu) + \delta_i^\mu (k \cdot q + m^2)), \quad (C20)$$

and $D_F^{ab}(k)$ is the free propagator. Here, we decompose the full vertex function into that at tree level and its correction, $\delta\Gamma_{i;abc}^\mu$:

$$\Gamma_{i;abc}^\mu(p, q, k) \equiv \Gamma_{(0)i;abc}^\mu(p, q, k) + \delta\Gamma_{i;abc}^\mu(p, q, k). \quad (C21)$$

Then, the correction to the vertex satisfies

$$ip_\mu \delta\Gamma_{i;cab}^\mu(p, q, k) = -ik_i X_{cb}^d \Pi_{da}(q) - iq_i X_c^d \Pi_{ab}(k). \quad (C22)$$

In the vacuum, Eq. (C22) gives the relation between the charge and wave function renormalization factors. In addition to that, at finite temperature, we will show that conserved charges are the collision invariants of the collision operator. To see this, we first take the limit $p \rightarrow \mathbf{0}$,

$$\begin{aligned}
ip_0 \delta\Gamma_{i;cab}^0(p, q, k) &= -ik_i (X_{cb}^d \Pi_{da}(q) - X_c^d \Pi_{db}(k)) \\
&\equiv F_{i;cab}(k, p^0). \quad (C23)
\end{aligned}$$

As we mentioned above, j_i^0 is a bilinear operator, so that the three-point vertex can be written by using the four-point vertex \mathcal{T}_{abcd} as

$$\begin{aligned}
\delta\Gamma_{i;cab}^0(p, q, k) &= \int \frac{d^4k'}{(2\pi)^4} (-i) \mathcal{T}_{abde}(q, k, -k', -q') \\
&\quad \times D^{fd}(k') D^{ge}(q') \Gamma_{(0)i;cgf}^0(p, q', k'), \quad (C24)
\end{aligned}$$

so that $F_{i;cab}(k, p^0)$ becomes

$$\begin{aligned}
& F_{i;cab}(k, p^0) \\
&= -i \int \frac{d^4k'}{(2\pi)^4} \mathcal{T}_{abde}(q, k, -k', -q') k'_i (X_c^d D^{ge}(q') \\
&\quad - X_{cf}^e D^{fd}(k') - D^{fd}(k') D^{ge}(k') F_{i;cgf}(k', p^0)) \quad (C25)
\end{aligned}$$

Let us define $\mathcal{T}^{(A)}_{abde}(q, k, -k', -q')$ by

$$\begin{aligned}
& \mathcal{T}_{abde}(q, k, -k', -q') \\
&= \mathcal{T}^{(A)}_{abde}(q, k, -k', -q') \\
&\quad + \int \frac{d^4k''}{(2\pi)^4} (-i) \mathcal{T}_{abd'e'}(q, k, -k'', -q'') \\
&\quad \times D^{b'd'}(k'') D^{a'e'}(q'') \mathcal{T}^{(A)}_{a'b'de}(q'', k'', -k', -q'). \quad (C26)
\end{aligned}$$

This is equivalent to Eq. (57) but in the standard basis. Comparing Eq. (C26) with Eq. (C25), we find

$$\begin{aligned}
F_{i;cab}(k, p^0) &= -i \int \frac{d^4k'}{(2\pi)^4} k'_i \mathcal{T}^{(A)}_{abde}(q, k, -k', -q') \\
&\quad \times (X_c^d D^{ge}(q') - X_{cf}^e D^{fd}(k')). \quad (C27)
\end{aligned}$$

We have derived Eq. (C27) in the standard basis; however, this is independent of a choice of basis. Now, let us apply it to the R/A basis. We take the case $a = b = A$ and $c = R$:

$$X_{RA}^R(p, q, k) = 1, \quad (C28)$$

$$X_{RA}^A(p, q, k) = 1 + f(p^0) + f(k^0), \quad (C29)$$

$$X_{RR}^R(p, q, k) = 1 + f(p^0) + f(q^0), \quad (C30)$$

$$X_{RR}^A(p, q, k) = 0. \quad (C31)$$

Therefore, $F_{i;RAA}$ becomes

$$\begin{aligned}
F_{i;RAA}(k, p^0) = & -i \int \frac{d^4 k'}{(2\pi)^4} k'_i [\mathcal{T}^{(A)}_{AARR}(-p-k, k, -k', p+k')(-i)(D^R(p+k') - D^A(k')) \\
& + \mathcal{T}^{(A)}_{AARA}(-p-k, k, -k', p+k')f(k^0)(-i)(D^A(p+k') - D^A(k')) \\
& - \mathcal{T}^{(A)}_{AAAR}(-p-k, k, -k', p+k')f(k^0 + p^0)(-i)(D^R(p+k') - D^R(k'))], \quad (C32)
\end{aligned}$$

where we have omitted $1 + f(p^0)$ in the second (third) term because there is no pole in the lower (upper) complex k^0 plane. Taking the limit $p^0 \rightarrow 0$, we find

$$\begin{aligned}
\lim_{p^0 \rightarrow 0} F_{i;RAA}(k, p^0) \\
= -i \int \frac{d^4 k'}{(2\pi)^4} k'_i \mathcal{T}^{(A)}_{AARR}(-k, k, -k', k') \rho(k'). \quad (C33)
\end{aligned}$$

On the other side, from Eq. (C23),

$$\begin{aligned}
F_{i;RAA}(k, p^0) = & -ik_i (X_{RA}^R(p, q, k) \Pi_{RA}(q) \\
& - X_{RA}^R(p, q, k) \Pi_{RA}(k)) \\
= & -ik_i (\Pi_A(q) - \Pi_A(k)). \quad (C34)
\end{aligned}$$

Taking $p^0 \rightarrow 0$, we find

$$\lim_{p^0 \rightarrow 0} F_{i;RAA}(k, p^0) = 2 \text{Im} \Pi_R(k) k_i. \quad (C35)$$

Inserting Eq. (C35) into Eq. (C33), we find

$$-2 \text{Im} \Pi_R(k) k_i + \int \frac{d^4 k'}{(2\pi)^4} \text{Im} \mathcal{T}^{(A)3}_3(k, k') \rho(k') k'_i = 0, \quad (C36)$$

where $\text{Im} \mathcal{T}^{(A)3}_3(k, k') = \text{Im} \mathcal{T}^{(A)}_{AARR}(-k, k, -k', k')$ is used. Using the collision operator, Eq. (77), we find

$$\mathcal{L} k_i = 0. \quad (C37)$$

Therefore, the conserved charge k_i is the zero mode of the collision operator.

-
- [1] J. Adams *et al.*, Nucl. Phys. **A757**, 102 (2005); K. Adcox *et al.*, *ibid.* **A757**, 184 (2005); I. Arsene *et al.*, *ibid.* **A757**, 1 (2005); B. B. Back *et al.*, *ibid.* **A757**, 28 (2005).
- [2] M. Gyulassy and L. McLerran, Nucl. Phys. **A750**, 30 (2005); A. Peshier and W. Cassing, Phys. Rev. Lett. **94**, 172301 (2005); B. Muller and J.L. Nagle, Annu. Rev. Nucl. Part. Sci. **56**, 93 (2006); S. Mrowczynski and M.H. Thoma, *ibid.* **57**, 61 (2007); E. V. Shuryak, Prog. Part. Nucl. Phys. **62**, 48 (2009); U. W. Heinz, arXiv:0901.4355.
- [3] R. D. Pisarski, Proc. Sci., LATTICE2008 (2008) 016.
- [4] P. Romatschke, Int. J. Mod. Phys. E **19**, 1 (2010); T. Schafer and D. Teaney, Rep. Prog. Phys. **72**, 126001 (2009); D. A. Teaney, arXiv:0905.2433, and references therein.
- [5] L. P. Csernai, J. I. Kapusta, and L. D. McLerran, Phys. Rev. Lett. **97**, 152303 (2006).
- [6] L. D. Landau and E. M. Lifshitz, *Physical Kinetics* (Pergamon, New York, 1981).
- [7] R. Kubo and K. Tomita, J. Phys. Soc. Jpn. **9**, 888 (1954); H. Nakano, Prog. Theor. Phys. **15**, 77 (1956); R. Kubo, J. Phys. Soc. Jpn. **12**, 570 (1957).
- [8] F. Karsch and H. W. Wyld, Phys. Rev. D **35**, 2518 (1987); A. Nakamura and S. Sakai, Phys. Rev. Lett. **94**, 072305 (2005); H. B. Meyer, Phys. Rev. D **76**, 101701 (2007); Phys. Rev. Lett. **100**, 162001 (2008); D. Kharzeev and K. Tuchin, J. High Energy Phys. 09 (2008) 093; F. Karsch, D. Kharzeev, and K. Tuchin, Phys. Lett. B **663**, 217 (2008).
- [9] K. Huebner, F. Karsch, and C. Pica, Phys. Rev. D **78**, 094501 (2008).
- [10] For the latest survey of the lattice calculations of transport coefficients, see H. B. Meyer, Nucl. Phys. **A830**, 641c (2009).
- [11] G. Policastro, D. T. Son, and A. O. Starinets, Phys. Rev. Lett. **87**, 081601 (2001); J. High Energy Phys. 09 (2002) 043; A. Buchel and J. T. Liu, Phys. Rev. Lett. **93**, 090602 (2004); P. Kovtun, D. T. Son, and A. O. Starinets, *ibid.* **94**, 111601 (2005); D. T. Son and A. O. Starinets, Annu. Rev. Nucl. Part. Sci. **57**, 95 (2007); R. Baier, P. Romatschke, D. T. Son, A. O. Starinets, and M. A. Stephanov, J. High Energy Phys. 04 (2008) 100; S. S. Gubser and A. Karch, Annu. Rev. Nucl. Part. Sci. **59**, 145 (2009).
- [12] S. S. Gubser and A. Nellore, Phys. Rev. D **78**, 086007 (2008); U. Gursoy, E. Kiritsis, L. Mazzanti, and F. Nitti, Phys. Rev. Lett. **101**, 181601 (2008); Nucl. Phys. **B820**, 148 (2009); N. Evans and E. Threlfall, Phys. Rev. D **78**, 105020 (2008); J. Noronha, M. Gyulassy, and G. Torrieri, Phys. Rev. Lett. **102**, 102301 (2009); Phys. Rev. C **82**, 054903 (2010); S. S. Gubser, S. S. Pufu, F. D. Rocha, and A. Yarom, arXiv:0902.4041; U. Gursoy, E. Kiritsis, G. Michalogiorgakis, and F. Nitti, J. High Energy Phys. 12 (2009) 056.
- [13] S. Jeon, Phys. Rev. D **52**, 3591 (1995); S. Jeon and L. G. Yaffe, *ibid.* **53**, 5799 (1996).
- [14] A. Hosoya, M. A. Sakagami, and M. Takao, Ann. Phys. (N.Y.) **154**, 229 (1984); E. Wang and U. W. Heinz, Phys. Lett. B **471**, 208 (1999); M. E. Carrington, D. f. Hou, and R. Kobes, Phys. Rev. D **62**, 025010 (2000); M. A. Valle Basagoiti, *ibid.* **66**, 045005 (2002); **67**, 025022 (2003); H.

- Defu, arXiv:hep-ph/0501284; D. Fernandez-Fraile, *Phys. Rev. D* **83**, 065001 (2011).
- [15] G. Aarts and J.M. Martinez Resco, *Phys. Rev. D* **68**, 085009 (2003); *J. High Energy Phys.* 02 (2004) 061; 03 (2005) 074; M.E. Carrington and E. Kovalchuk, *Phys. Rev. D* **76**, 045019 (2007).
- [16] M.E. Carrington and E. Kovalchuk, *Phys. Rev. D* **77**, 025015 (2008); **80**, 085013 (2009).
- [17] J. S. Gagnon and S. Jeon, *Phys. Rev. D* **75**, 025014 (2007); **76**, 089902(E) (2007); **76**, 105019 (2007).
- [18] S. Gavin, *Nucl. Phys.* **A435**, 826 (1985); M. Prakash, M. Prakash, R. Venugopalan, and G. Welke, *Phys. Rep.* **227**, 321 (1993); D. Davesne, *Phys. Rev. C* **53**, 3069 (1996); A. Dobado and S.N. Santalla, *Phys. Rev. D* **65**, 096011 (2002); A. Dobado and F.J. Llanes-Estrada, *ibid.* **69**, 116004 (2004); D. Fernandez-Fraile and A. Gomez Nicola, *ibid.* **73**, 045025 (2006); J.W. Chen and E. Nakano, *Phys. Lett. B* **647**, 371 (2007); J.W. Chen, Y.H. Li, Y.F. Liu, and E. Nakano, *Phys. Rev. D* **76**, 114011 (2007); K. Itakura, O. Morimatsu, and H. Otomo, *ibid.* **77**, 014014 (2008); J.W. Chen and J. Wang, *Phys. Rev. C* **79**, 044913 (2009); D. Fernandez-Fraile and A.G. Nicola, *Phys. Rev. Lett.* **102**, 121601 (2009); C. Sasaki and K. Redlich, *Phys. Rev. C* **79**, 055207 (2009); *Nucl. Phys.* **A832**, 62 (2010); P. Chakraborty and J.I. Kapusta, *Phys. Rev. C* **83**, 014906 (2011).
- [19] U. W. Heinz, *Phys. Rev. Lett.* **51**, 351 (1983); *Ann. Phys. (N.Y.)* **161**, 48 (1985); **168**, 148 (1986); A. Hosoya and K. Kajantie, *Nucl. Phys.* **B250**, 666 (1985); G. Baym, H. Monien, C.J. Pethick, and D.G. Ravenhall, *Phys. Rev. Lett.* **64**, 1867 (1990); M.H. Thoma, *Phys. Lett. B* **269**, 144 (1991); D. W. von Oertzen, *ibid.* **280**, 103 (1992); H. Heiselberg, *Phys. Rev. D* **49**, 4739 (1994); *Phys. Rev. Lett.* **72**, 3013 (1994); G. Baym and H. Heiselberg, *Phys. Rev. D* **56**, 5254 (1997); J. Ahonen, *ibid.* **59**, 023004 (1998); M. Asakawa, S. A. Bass, and B. Muller, *Phys. Rev. Lett.* **96**, 252301 (2006); *Prog. Theor. Phys.* **116**, 725 (2006); Z. Xu and C. Greiner, *Phys. Rev. Lett.* **100**, 172301 (2008); M. A. York and G.D. Moore, *Phys. Rev. D* **79**, 054011 (2009); J.W. Chen, H. Dong, K. Ohnishi, and Q. Wang, *Phys. Lett. B* **685**, 277 (2010).
- [20] P. Arnold, G.D. Moore, and L. G. Yaffe, *J. High Energy Phys.* 11 (2000) 001; 05 (2003) 051.
- [21] Y. Hidaka and R.D. Pisarski, *Phys. Rev. D* **78**, 071501 (2008); **80**, 036004 (2009); **80**, 074504 (2009); **81**, 076002 (2010).
- [22] G.D. Moore, *Phys. Rev. D* **76**, 107702 (2007).
- [23] M.E. Carrington and E. Kovalchuk, *Phys. Rev. D* **81**, 065017 (2010).
- [24] G.M. Eliashberg, *Sov. Phys. JETP* **14**, 886 (1962).
- [25] M. Le Bellac, *Thermal Field Theory* (Cambridge University Press, Cambridge, England, 2000).
- [26] P. Aurenche and T. Becherroway, *Nucl. Phys.* **B379**, 259 (1992).
- [27] M. A. van Eijck, R. Kobes, and C.G. van Weert, *Phys. Rev. D* **50**, 4097 (1994).
- [28] F. Gelis, D. Schiff, and J. Serreau, *Phys. Rev. D* **64**, 056006 (2001).
- [29] S. Chapman and T. G. Cowling, *The Mathematical Theory of Non-Uniform Gases* (Cambridge University Press, Cambridge, England, 1970), 3rd ed..
- [30] T. Koide, E. Nakano, and T. Kodama, *Phys. Rev. Lett.* **103**, 052301 (2009).
- [31] T. Altherr, *Phys. Lett. B* **238**, 360 (1990).
- [32] Y. Hidaka and T. Kunihiro (unpublished).
- [33] L.D. Landau and I. Pomeranchuk, *Dokl. Akad. Nauk SSSR* **92**, 535 (1953); **92**, 735 (1953); A.B. Migdal, *ibid.* **105**, 77 (1955); *Phys. Rev.* **103**, 1811 (1956).
- [34] P. B. Arnold, G. D. Moore, and L. G. Yaffe, *J. High Energy Phys.* 01 (2003) 030.
- [35] R.L. Kobes and G.W. Semenoff, *Nucl. Phys.* **B260**, 714 (1985); **B272**, 329 (1986).
- [36] T. Toyoda, *Ann. Phys. (N.Y.)* **173**, 226 (1987).
- [37] G. Aarts and J.M. Martinez Resco, *J. High Energy Phys.* 11 (2002) 022.